Microscopic calculation of the ^{3}He(α,γ)^{7}Be capture reaction in the FMD approach

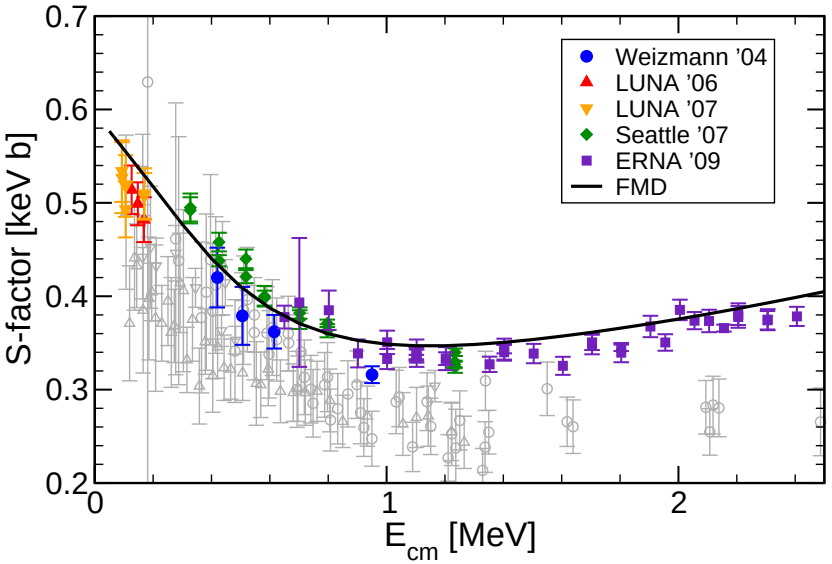

Thomas Neff

"Interfaces between structure and reactions"

INT, Seattle

Aug 17, 2011

HELMHOLTZ ASSOCIATION

GSI

Overview

Effective Nucleon-Nucleon interaction:

Unitary Correlation Operator Method

R. Roth, T. Neff, H. Feldmeier, Prog. Part. Nucl. Phys. 65 (2010) 50

- **Short-range Correlations and Effective Interaction**
- **NCSM calculations**

Many-Body Method:

Fermionic Molecular Dynamics

- **Model**
- **^{3}He(α,γ)^{7}Be Radiative Capture Reaction**

T. Neff, Phys. Rev. Lett. 106, 042502 (2011)

Nuclear Force

Argonne V18 (T=0)

spins aligned parallel or perpendicular to the relative distance vector

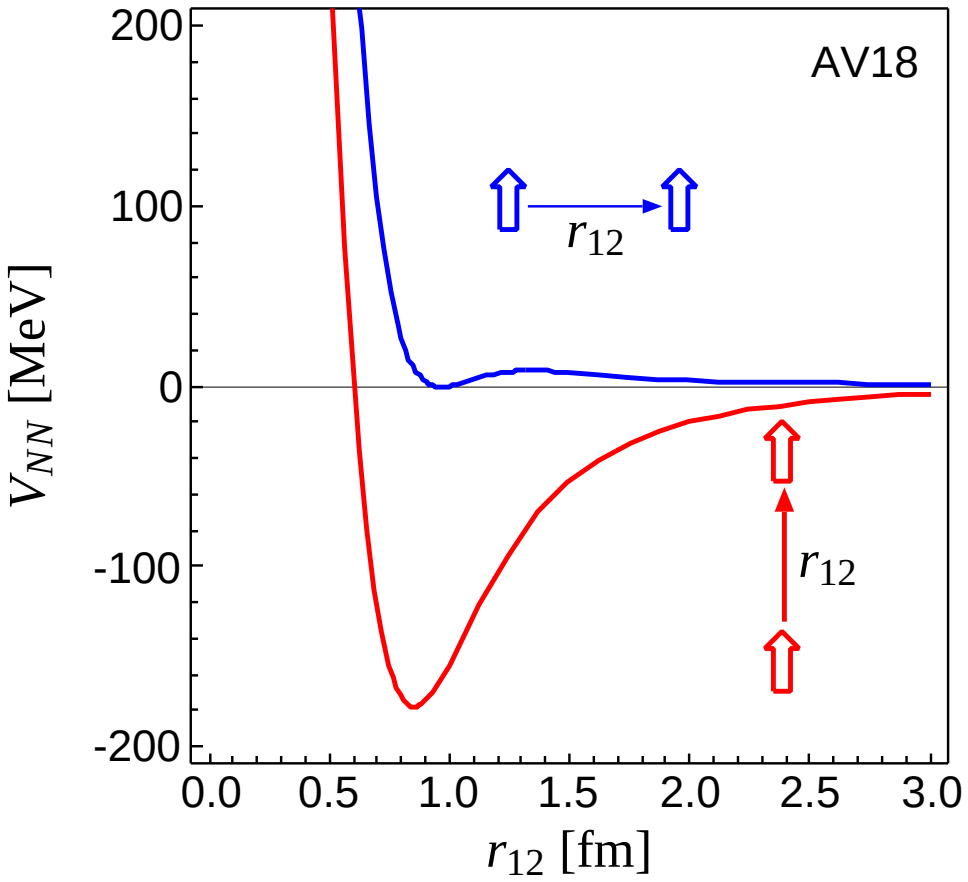

- strong repulsive core: nucleons can not get closer than ≈ 0.5 fm

➨ **central correlations**

- strong dependence on the orientation of the spins due to the tensor force

➨ **tensor correlations**

Nuclear Force

Argonne V18 (T=0)

spins aligned parallel or perpendicular to the relative distance vector

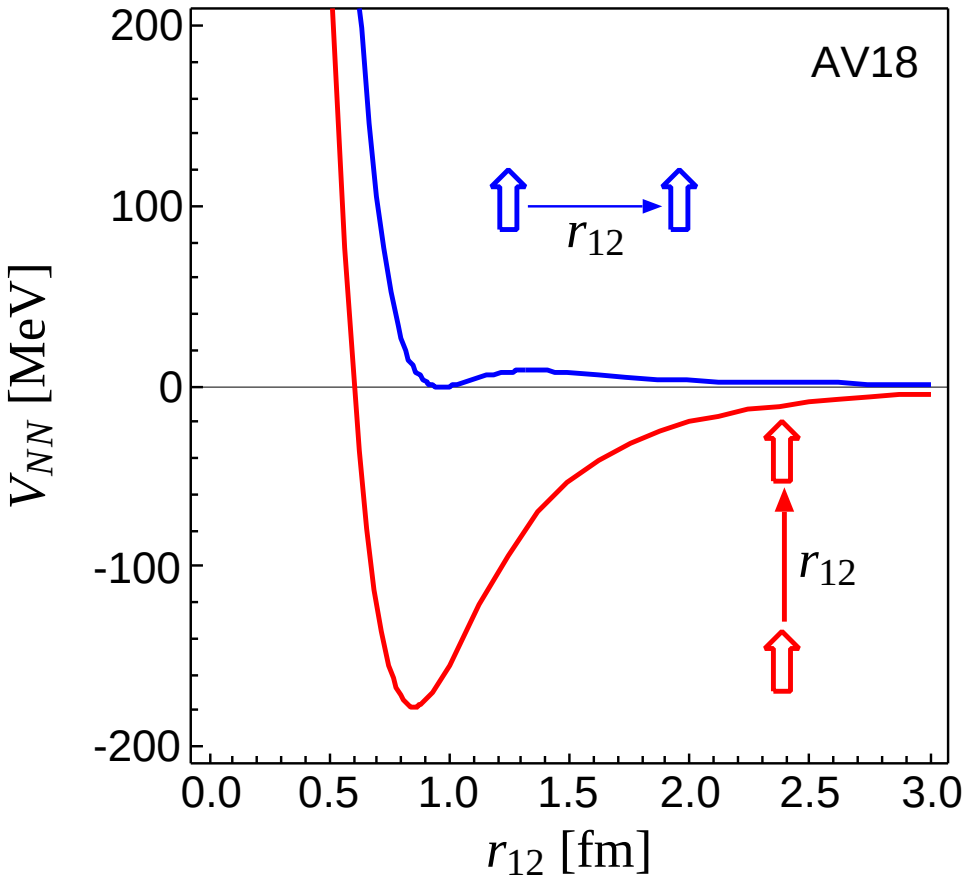

- strong repulsive core: nucleons can not get closer than ≈ 0.5 fm

➨ **central correlations**

- strong dependence on the orientation of the spins due to the tensor force

➨ **tensor correlations**

the nuclear force will induce **strong short-range correlations** in the nuclear wave function

One-body densities

coordinate space

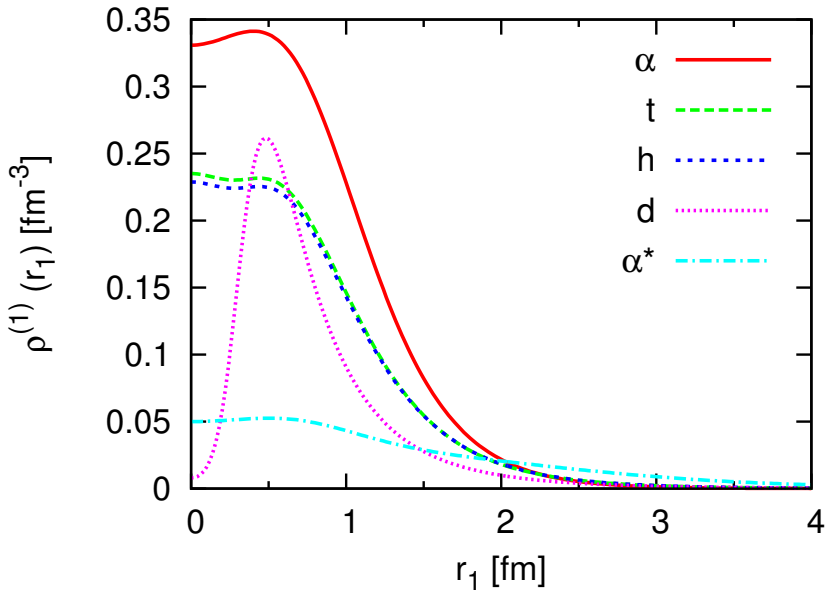

momentum space

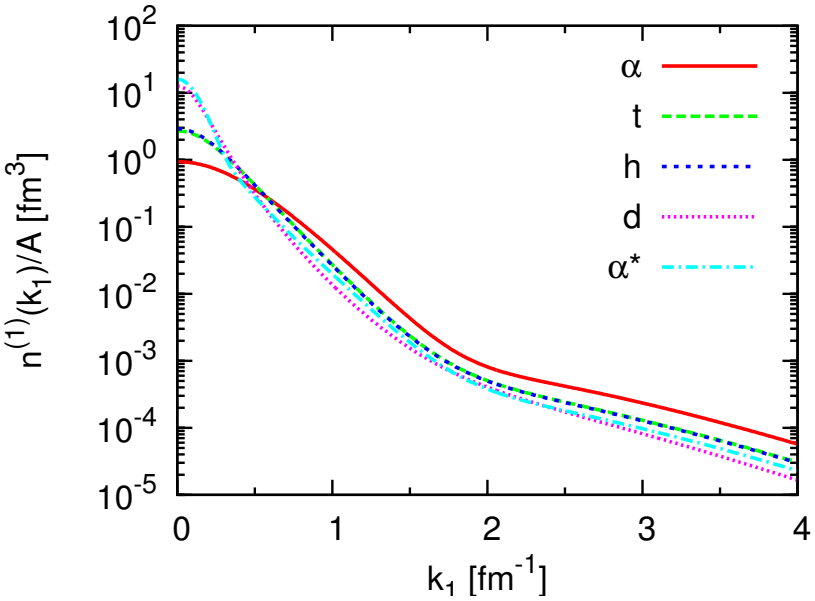

- one-body densities calculated from exact wave functions for AV8' interaction
- coordinate space densities reflect different sizes and densities of ^{2}H, ^{3}H, ^{3}He, ^{4}He and the 0_2^+ state in ^{4}He
- similar high-momentum tails in the momentum densities

Feldmeier, Horiuchi, Neff, Suzuki, arXiv:1107.4956

Two-body densities

coordinate space

$S = 1, M_S = 1, T = 0$

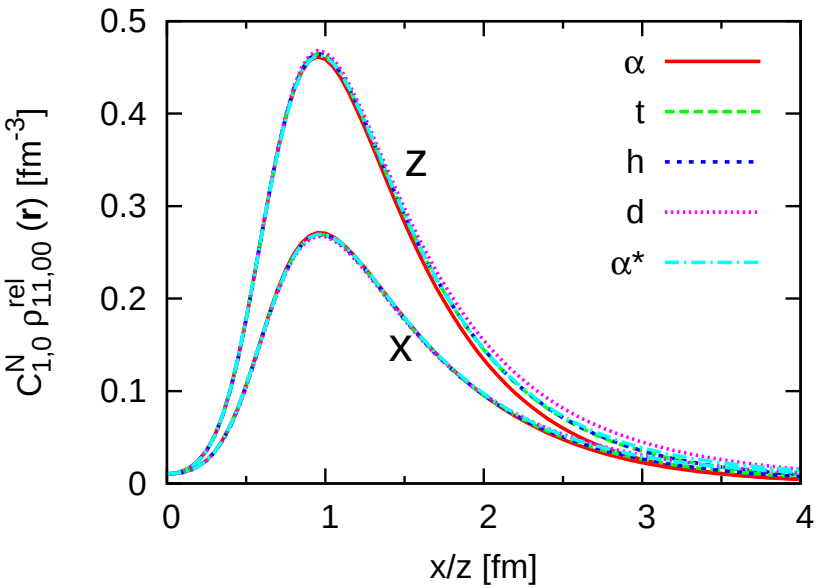

momentum space

$S = 1, T = 0$

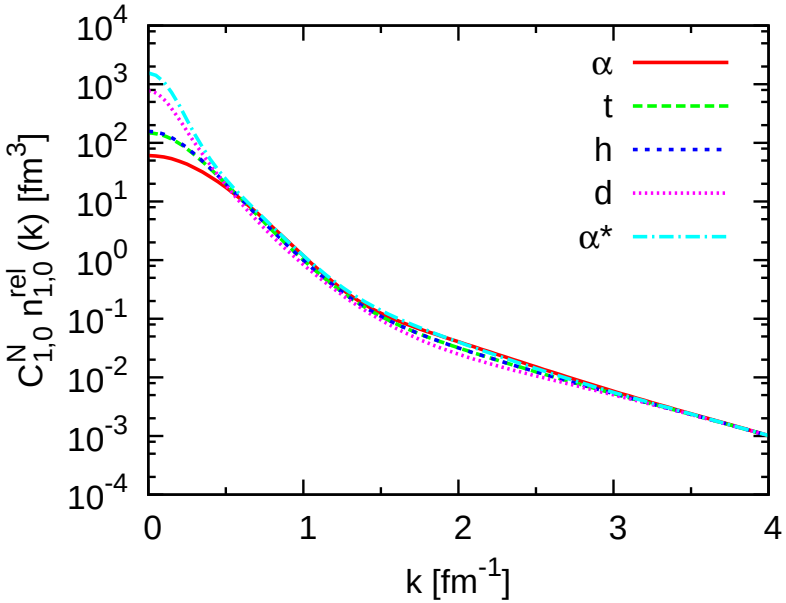

- normalize two-body density in coordinate space at r=1.0 fm
- normalized two-body densities in coordinate are identical at short distances for all nuclei
- use the **same** normalization factor in momentum space – high momentum tails agree for all nuclei

Feldmeier, Horiuchi, Neff, Suzuki, arXiv:1107.4956

UCOM

Unitary Correlation Operator Method

Correlation Operator

- induce short-range (two-body) central and tensor correlations into the many-body state

$$\underset{\sim}{C} = \underset{\sim}{C}_\Omega \underset{\sim}{C}_r = \exp\Big[-i \sum_{i<j} \underset{\sim}{g}_{\Omega,ij}\Big] \exp\Big[-i \sum_{i<j} \underset{\sim}{g}_{r,ij}\Big] \quad , \quad \underset{\sim}{C}^\dagger \underset{\sim}{C} = \underset{\sim}{1}$$

- correlation operator should conserve the symmetries of the Hamiltonian and should be of finite-range, correlated interaction **phase shift equivalent** to bare interaction by construction

Correlated Operators

- correlated operators will have contributions in higher cluster orders

$$\underset{\sim}{C}^\dagger \underset{\sim}{O} \underset{\sim}{C} = \underset{\sim}{\hat{O}}^{[1]} + \underset{\sim}{\hat{O}}^{[2]} + \underset{\sim}{\hat{O}}^{[3]} + \ldots$$

- two-body approximation: correlation range should be small compared to mean particle distance

Correlated Interaction

$$\underset{\sim}{C}^\dagger (\underset{\sim}{T} + \underset{\sim}{V}) \underset{\sim}{C} = \underset{\sim}{T} + \underset{\sim}{V}_{\mathrm{UCOM}} + \underset{\sim}{V}^{[3]}_{\mathrm{UCOM}} + \ldots$$

UCOM

Central and Tensor Correlations

$$\underset{\sim}{C} = \underset{\sim}{C}_\Omega \underset{\sim}{C}_r$$

$$\mathbf{p} = \mathbf{p}_r + \mathbf{p}_\Omega$$

$$\mathbf{p}_r = \frac{1}{2}\left\{\frac{\mathbf{r}}{r}\left(\frac{\mathbf{r}}{r}\mathbf{p}\right) + \left(\mathbf{p}\frac{\mathbf{r}}{r}\right)\frac{\mathbf{r}}{r}\right\}, \qquad \mathbf{p}_\Omega = \frac{1}{2r}\left\{\mathbf{l} \times \frac{\mathbf{r}}{r} - \frac{\mathbf{r}}{r} \times \mathbf{l}\right\}$$

UCOM

Central and Tensor Correlations

$$\underset{\sim}{C} = \underset{\sim}{C}_\Omega \underset{\sim}{C}_r$$

$$\mathbf{p} = \mathbf{p}_r + \mathbf{p}_\Omega$$

$$\mathbf{p}_r = \frac{1}{2}\left\{\frac{\mathbf{r}}{r}\left(\frac{\mathbf{r}}{r}\mathbf{p}\right) + \left(\mathbf{p}\frac{\mathbf{r}}{r}\right)\frac{\mathbf{r}}{r}\right\}, \qquad \mathbf{p}_\Omega = \frac{1}{2r}\left\{\mathbf{l}\times\frac{\mathbf{r}}{r} - \frac{\mathbf{r}}{r}\times\mathbf{l}\right\}$$

Central Correlations

$$\underset{\sim}{c}_r = \exp\left\{-\frac{i}{2}\{p_r s(r) + s(r) p_r\}\right\}$$

- probability density shifted out of the repulsive core

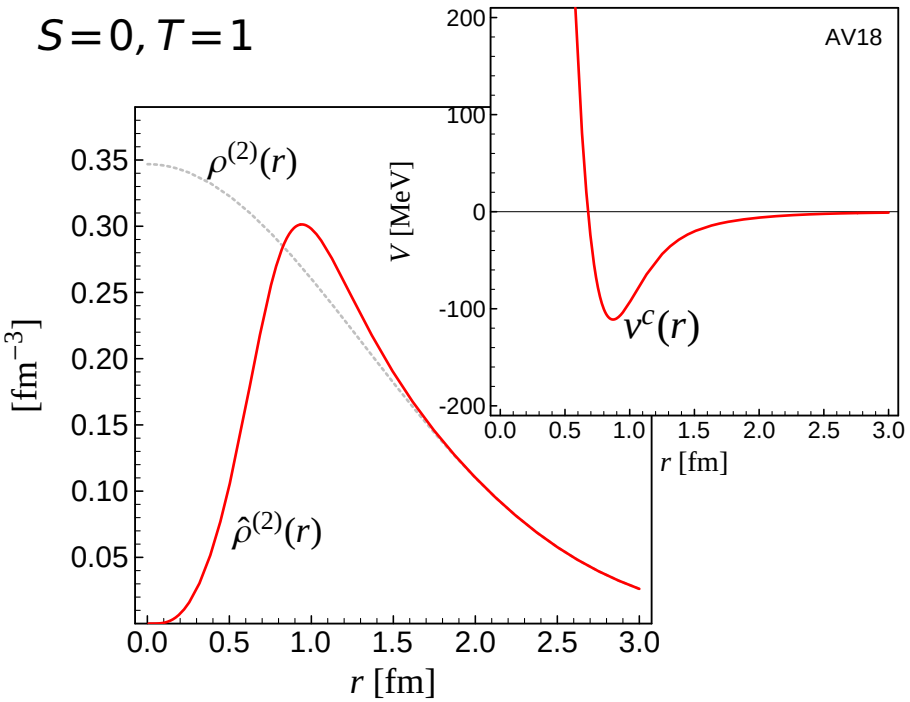

UCOM

Central and Tensor Correlations

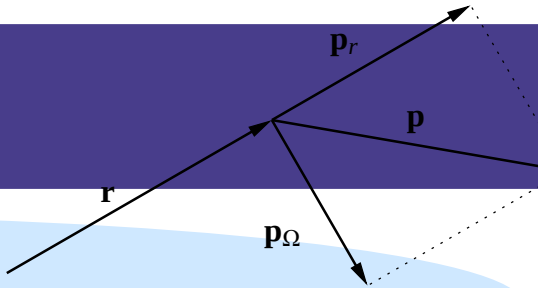

$$\underset{\sim}{C} = \underset{\sim}{C}_\Omega \underset{\sim}{C}_r$$

$$\mathbf{p} = \mathbf{p}_r + \mathbf{p}_\Omega$$

$$\mathbf{p}_r = \tfrac{1}{2}\left\{\frac{\mathbf{r}}{r}\left(\frac{\mathbf{r}}{r}\mathbf{p}\right) + \left(\mathbf{p}\frac{\mathbf{r}}{r}\right)\frac{\mathbf{r}}{r}\right\}, \qquad \mathbf{p}_\Omega = \frac{1}{2r}\left\{\mathbf{l}\times\frac{\mathbf{r}}{r} - \frac{\mathbf{r}}{r}\times\mathbf{l}\right\}$$

Central Correlations

$$\underset{\sim}{c}_r = \exp\left\{-\tfrac{i}{2}\{p_r s(r) + s(r) p_r\}\right\}$$

- probability density shifted out of the repulsive core

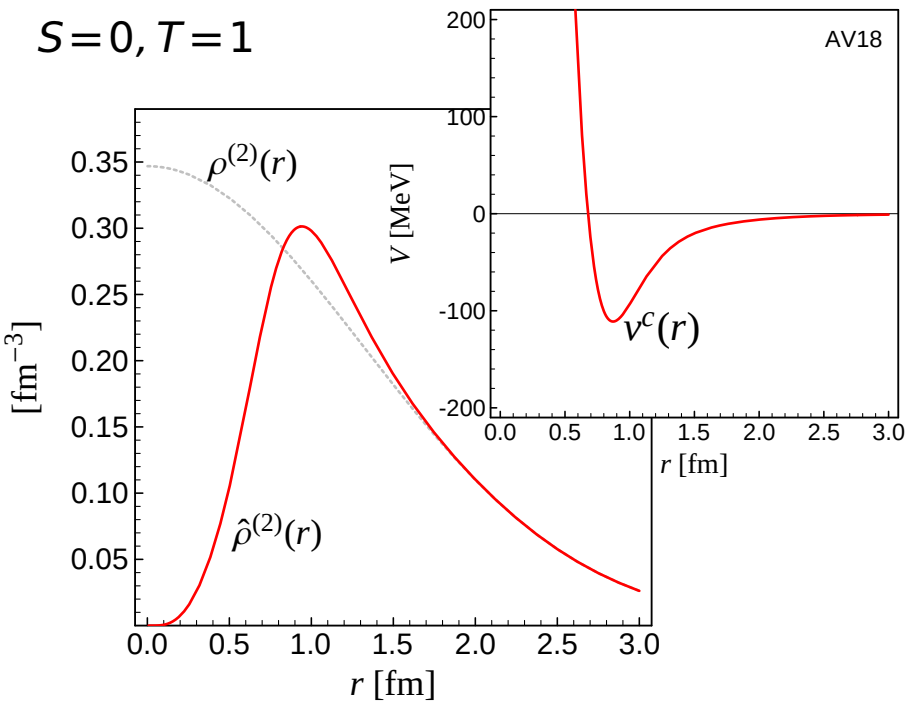

Tensor Correlations

$$\underset{\sim}{c}_\Omega = \exp\left\{-i\vartheta(r)\left\{\tfrac{3}{2}(\boldsymbol{\sigma}_1\cdot\mathbf{p}_\Omega)(\boldsymbol{\sigma}_2\cdot\mathbf{r}) + \tfrac{3}{2}(\boldsymbol{\sigma}_1\cdot\mathbf{r})(\boldsymbol{\sigma}_2\cdot\mathbf{p}_\Omega)\right\}\right.$$

- tensor force admixes other angular momenta

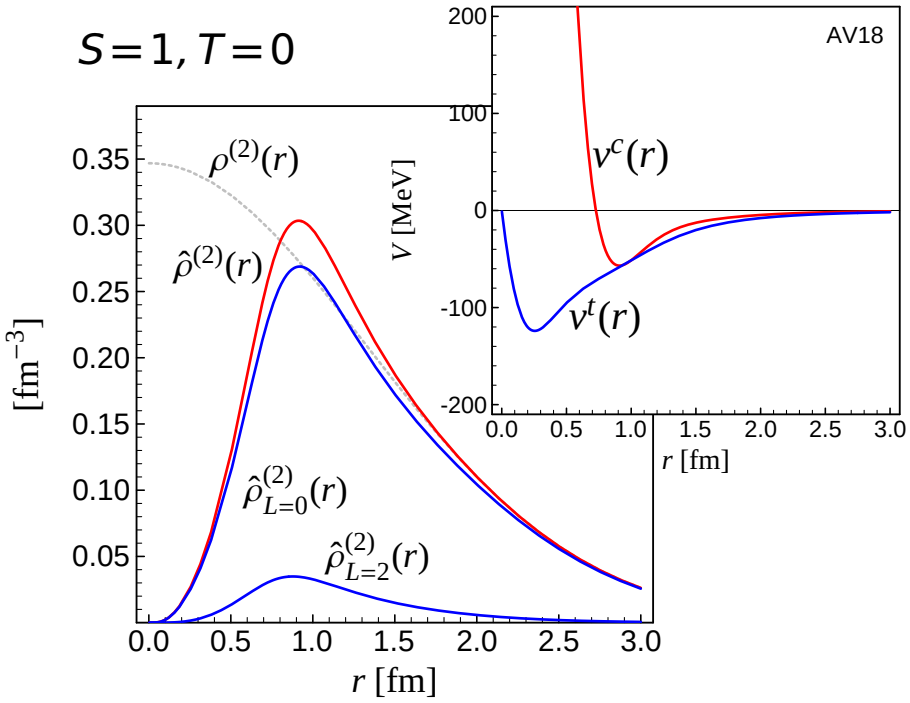

UCOM

Central and Tensor Correlations

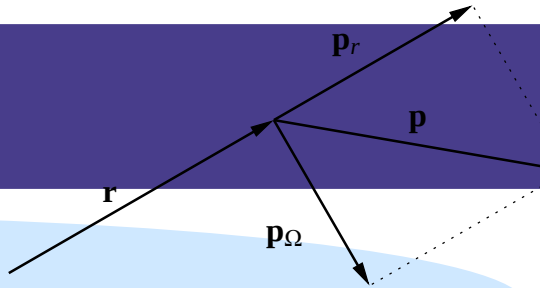

$$\underset{\sim}{C} = \underset{\sim}{C}_\Omega \underset{\sim}{C}_r$$

$$\mathbf{p} = \mathbf{p}_r + \mathbf{p}_\Omega$$

$$\mathbf{p}_r = \tfrac{1}{2}\left\{\frac{\mathbf{r}}{r}\left(\frac{\mathbf{r}}{r}\mathbf{p}\right) + \left(\mathbf{p}\frac{\mathbf{r}}{r}\right)\frac{\mathbf{r}}{r}\right\}, \qquad \mathbf{p}_\Omega = \frac{1}{2r}\left\{\mathbf{l}\times\frac{\mathbf{r}}{r} - \frac{\mathbf{r}}{r}\times\mathbf{l}\right\}$$

Central Correlations

$$\underset{\sim}{c}_r = \exp\left\{-\tfrac{i}{2}\{p_r s(r) + s(r) p_r\}\right\}$$

- probability density shifted out of the repulsive core

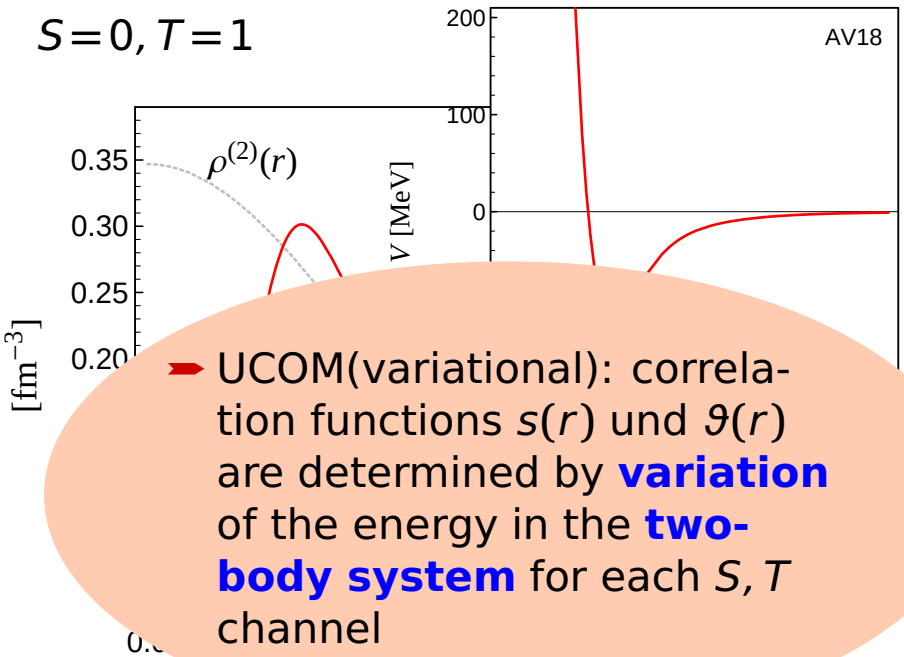

- UCOM(variational): correlation functions $s(r)$ und $\vartheta(r)$ are determined by **variation** of the energy in the **two-body system** for each S, T channel

Tensor Correlations

$$\underset{\sim}{c}_\Omega = \exp\left\{-i\vartheta(r)\left\{\tfrac{3}{2}(\boldsymbol{\sigma}_1\cdot\mathbf{p}_\Omega)(\boldsymbol{\sigma}_2\cdot\mathbf{r}) + \tfrac{3}{2}(\boldsymbol{\sigma}_1\cdot\mathbf{r})(\boldsymbol{\sigma}_2\cdot\mathbf{p}_\Omega)\right\}\right.$$

- tensor force admixes other angular momenta

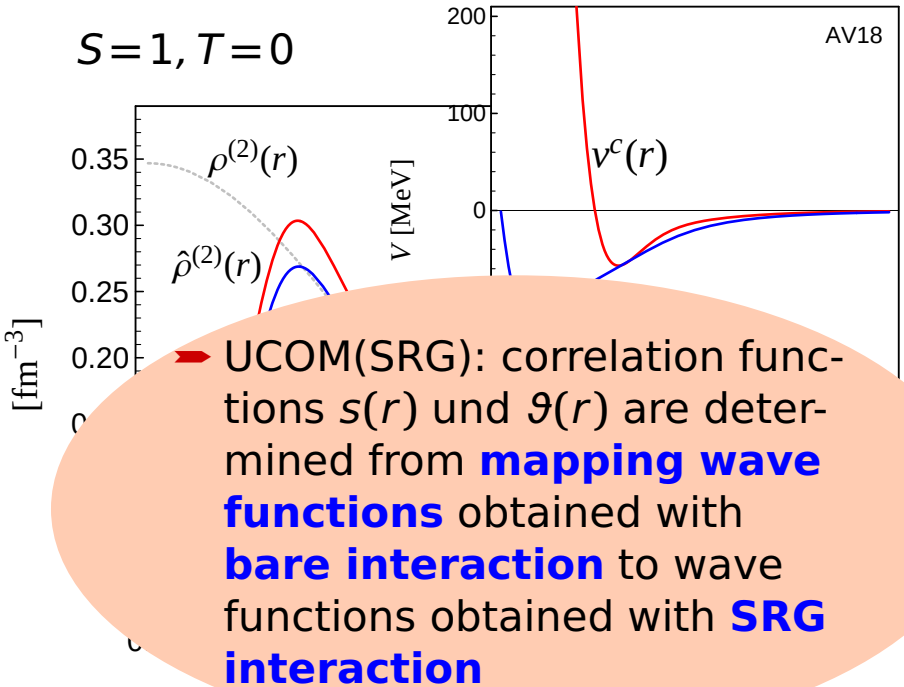

- UCOM(SRG): correlation functions $s(r)$ und $\vartheta(r)$ are determined from **mapping wave functions** obtained with **bare interaction** to wave functions obtained with **SRG interaction**

Correlations and Energies

two-body densities

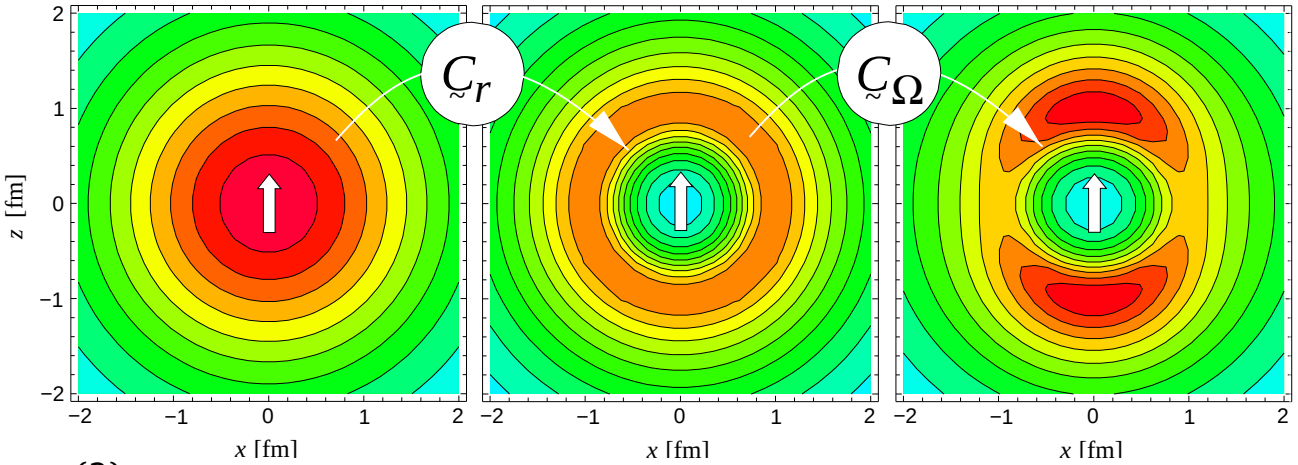

$\rho^{(2)}_{S,T}(\mathbf{r}_1 - \mathbf{r}_2) \quad S = 1, M_S = 1, T = 0$

central correlator C_r shifts density out of the repulsive core

tensor correlator C_Ω aligns density with spin orientation

Neff and Feldmeier, Nucl. Phys. **A713** (2003) 311

Correlations and Energies

two-body densities

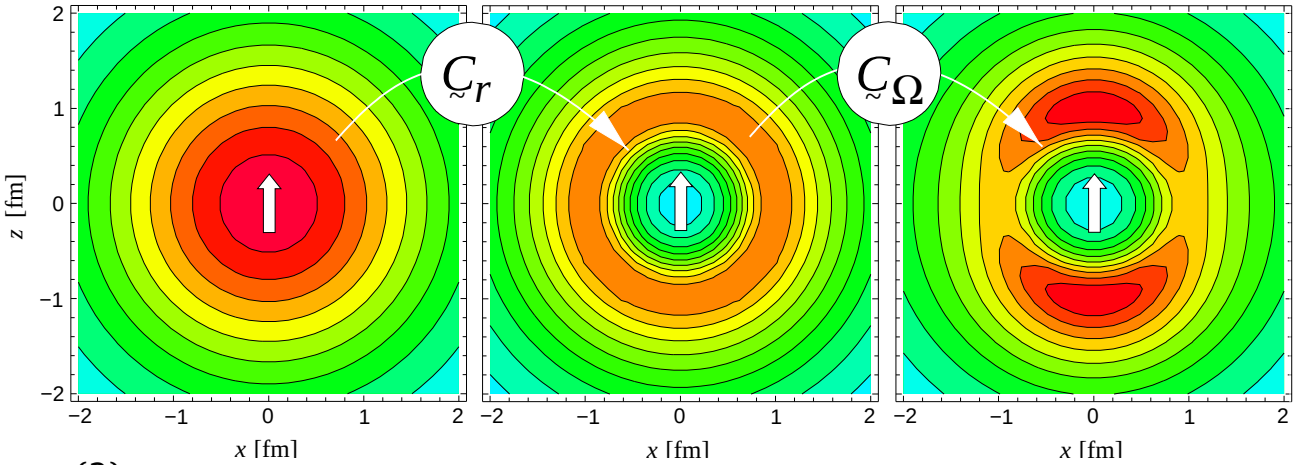

$\rho^{(2)}_{S,T}(\mathbf{r}_1 - \mathbf{r}_2) \quad S = 1, M_S = 1, T = 0$

central correlator C_r shifts density out of the repulsive core

tensor correlator C_Ω aligns density with spin orientation

both central and tensor correlations are essential for binding

energies

$0\hbar\omega$ Harmonic Oscillator

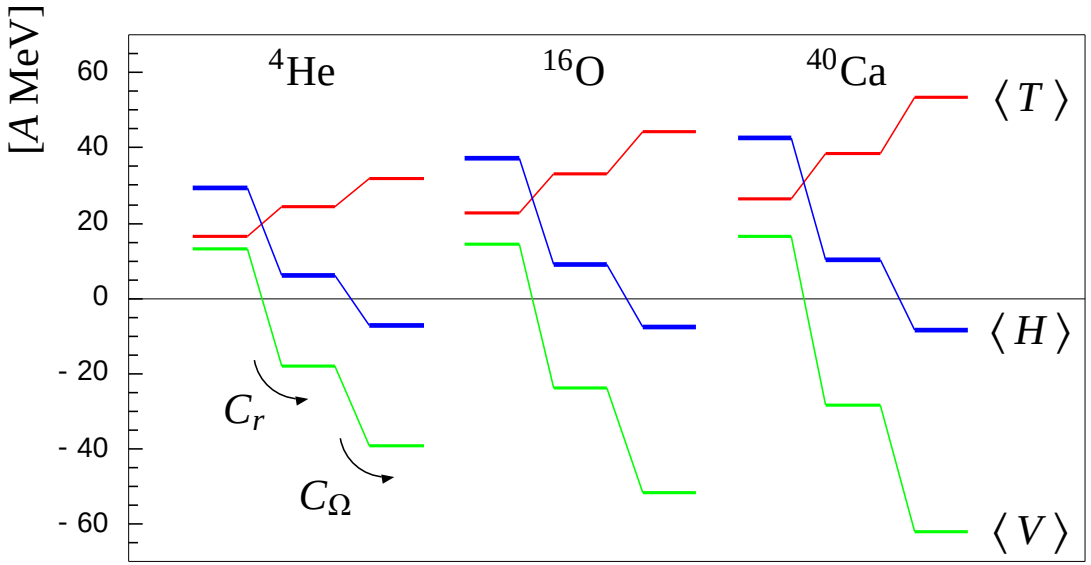

Neff and Feldmeier, Nucl. Phys. **A713** (2003) 311

Two-body Densities

coordinate space

$S = 1, M_S = 1, T = 0$

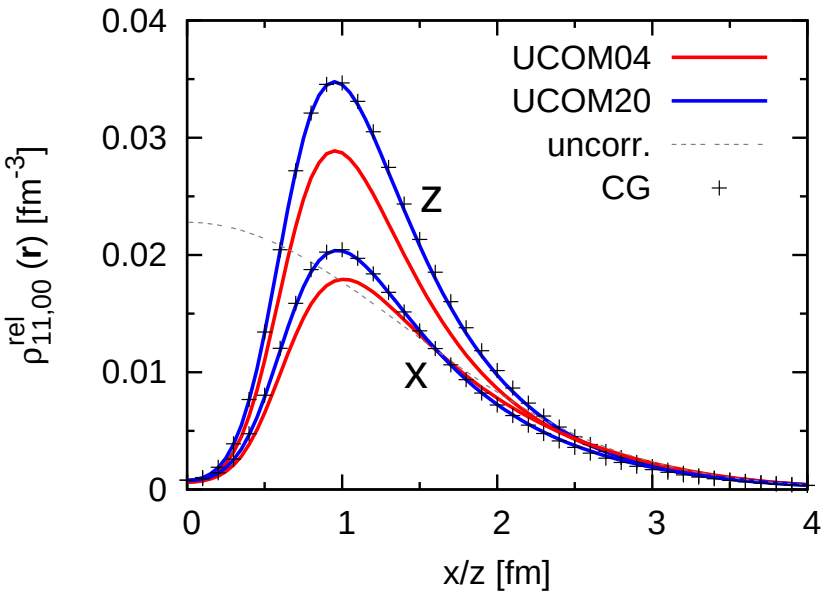

momentum space

$S = 1, T = 0$

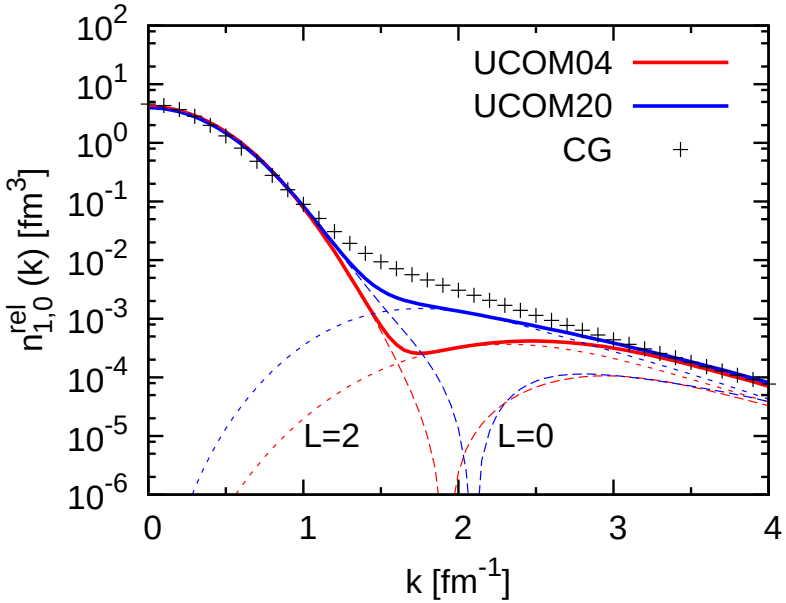

- two-body densities calculated from $0\hbar\Omega$ ^{4}He and correlated density operators
- UCOM20 correlators derived from $\lambda \approx 1.5$ fm^{-1} SRG interaction reproduce coordinate space two-body density and high-momentum components very well
- high-momentum components dominated by tensor correlations
- long-range correlations should fill up momentum space two-body density above the Fermi momentum

Feldmeier, Horiuchi, Neff, Suzuki, arXiv:1107.4956

Unitary Correlation Operator Method

Correlated Interaction in Momentum Space

$^3S_1$ bare

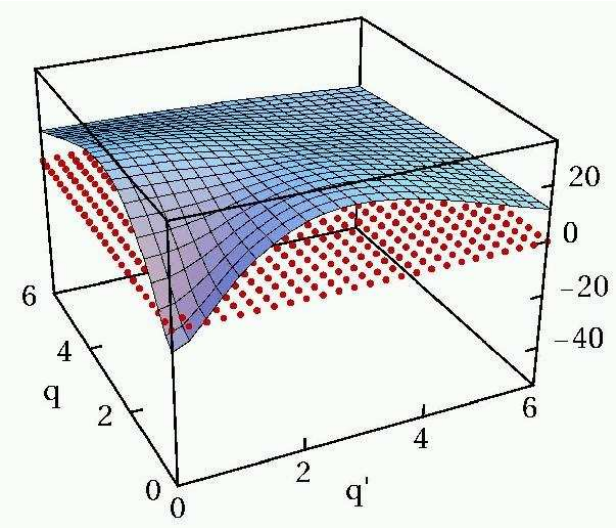

bare interaction has **strong off-diagonal** matrix elements connecting to high momenta

$^3S_1$ - $^3D_1$ bare

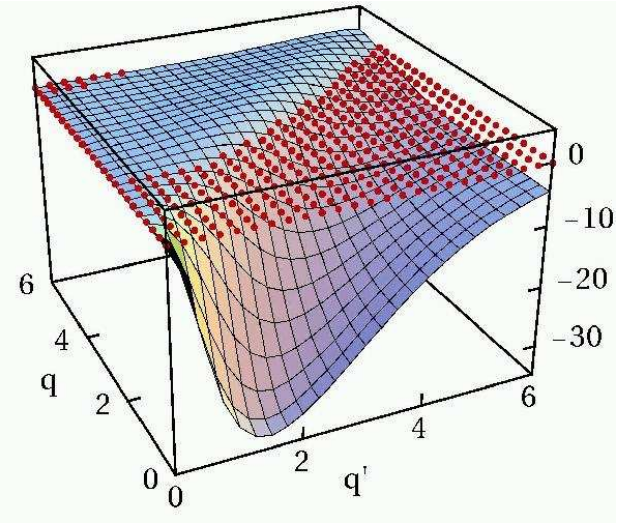

Roth, Hergert, Papakonstaninou, Neff, Feldmeier, Phys. Rev. C **72**, 034002 (2005)

Unitary Correlation Operator Method

Correlated Interaction in Momentum Space

$^3S_1$ bare

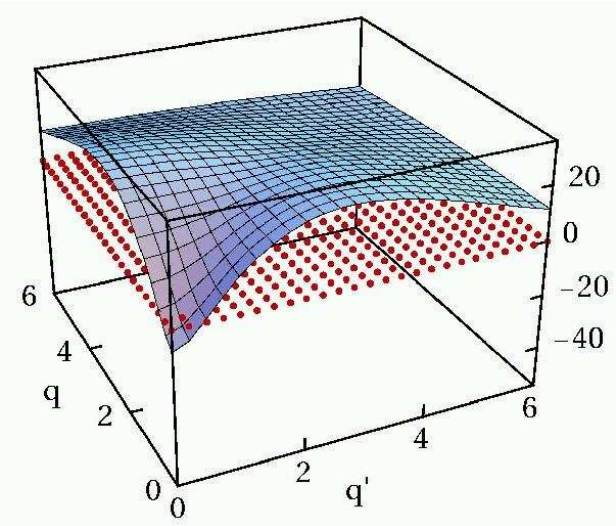

bare interaction has **strong off-diagonal** matrix elements connecting to high momenta

$^3S_1$ - $^3D_1$ bare

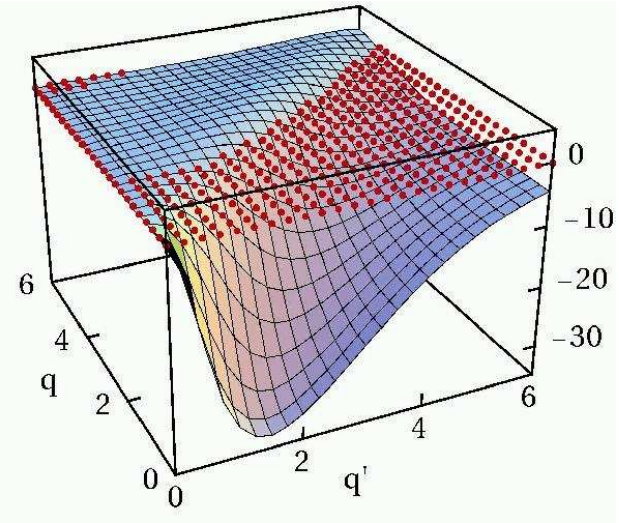

$^3S_1$ correlated

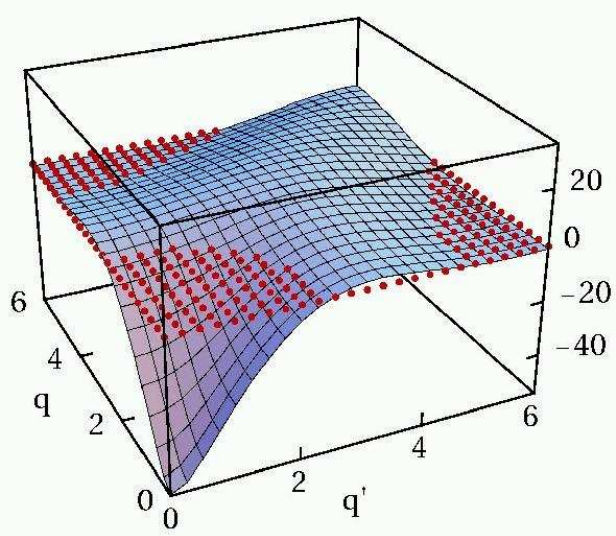

correlated interaction is **more attractive** at low momenta

$^3S_1$ - $^3D_1$ correlated

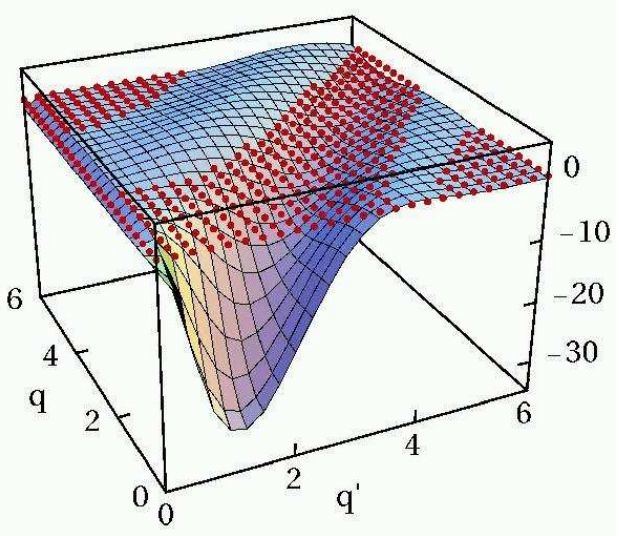

off-diagonal matrix elements connecting low- and high- momentum states are **strongly reduced**

Roth, Hergert, Papakonstaninou, Neff, Feldmeier, Phys. Rev. C **72**, 034002 (2005)

Correlated Interaction in Momentum Space

$^3S_1$ bare

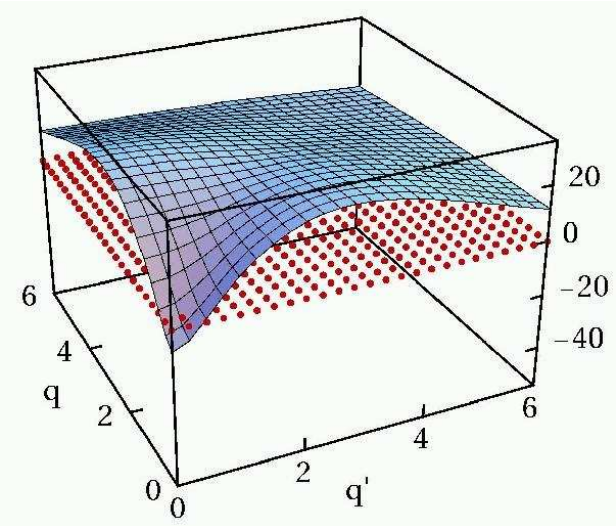

bare interaction has **strong off-diagonal** matrix elements connecting to high momenta

$^3S_1$ - $^3D_1$ bare

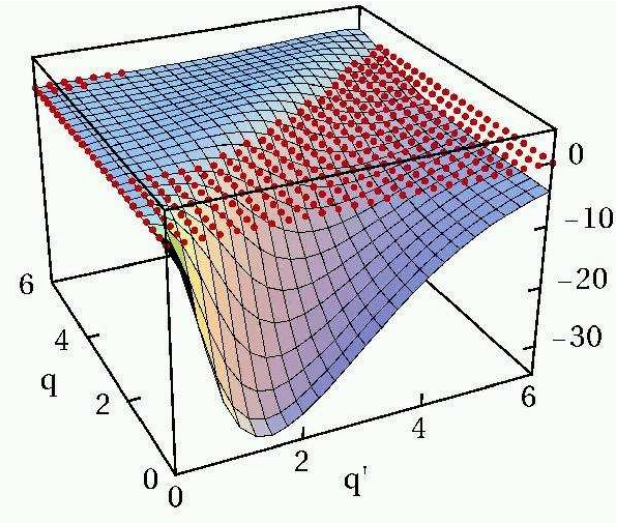

$^3S_1$ correlated

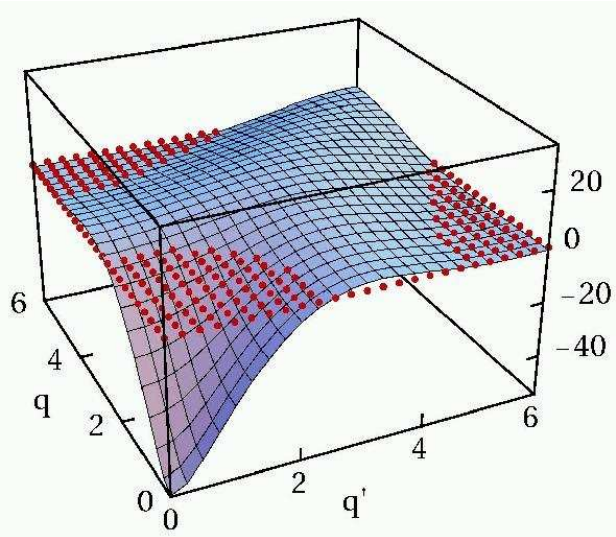

correlated interaction is **more attractive** at low momenta

off-diagonal matrix elements connecting low- and high- momentum states are **strongly reduced**

$^3S_1$ - $^3D_1$ correlated

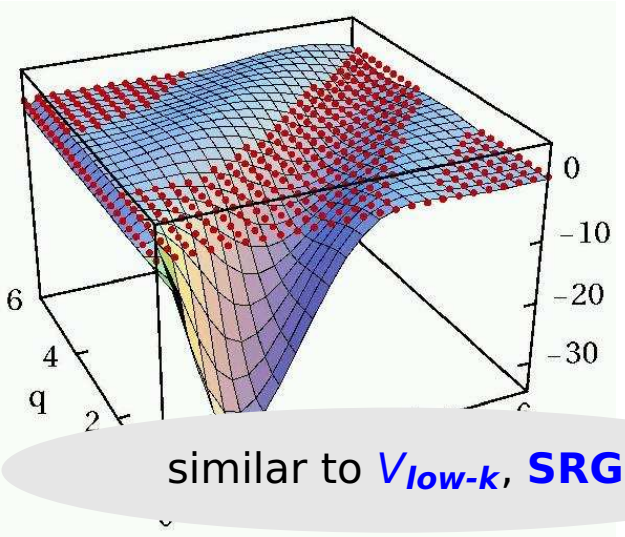

similar to $V_{low\text{-}k}$, **SRG**

Roth, Hergert, Papakonstaninou, Neff, Feldmeier, Phys. Rev. C **72**, 034002 (2005)

UCOM(SRG)

No-Core Shell Model Calculations

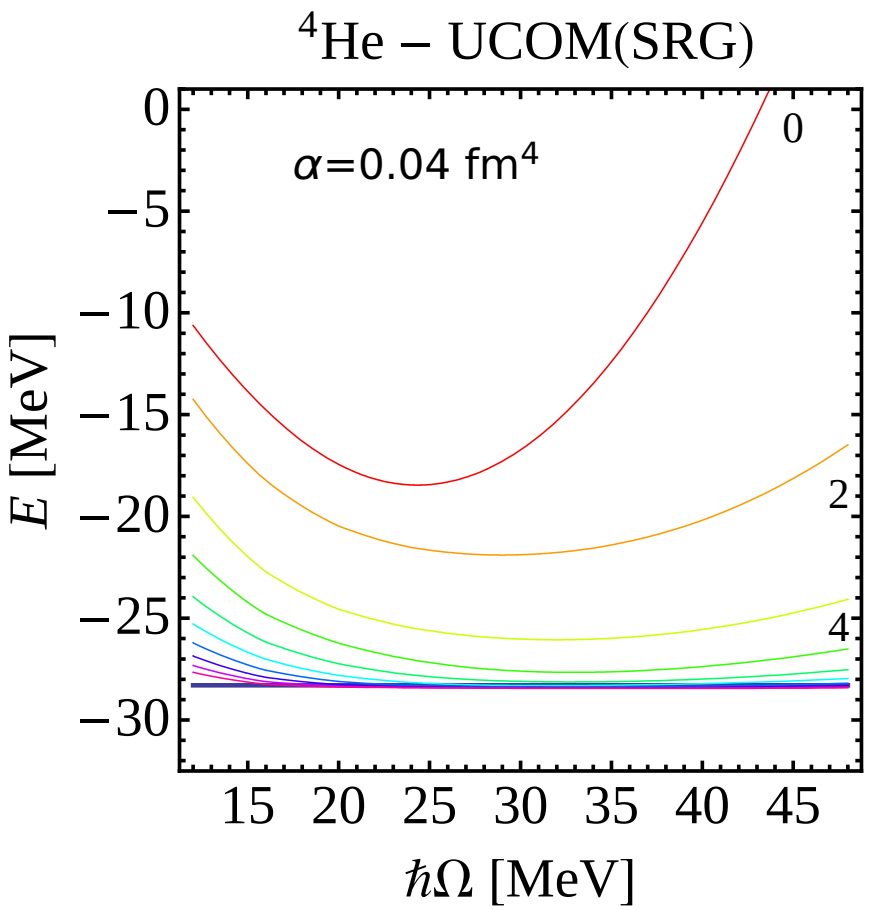

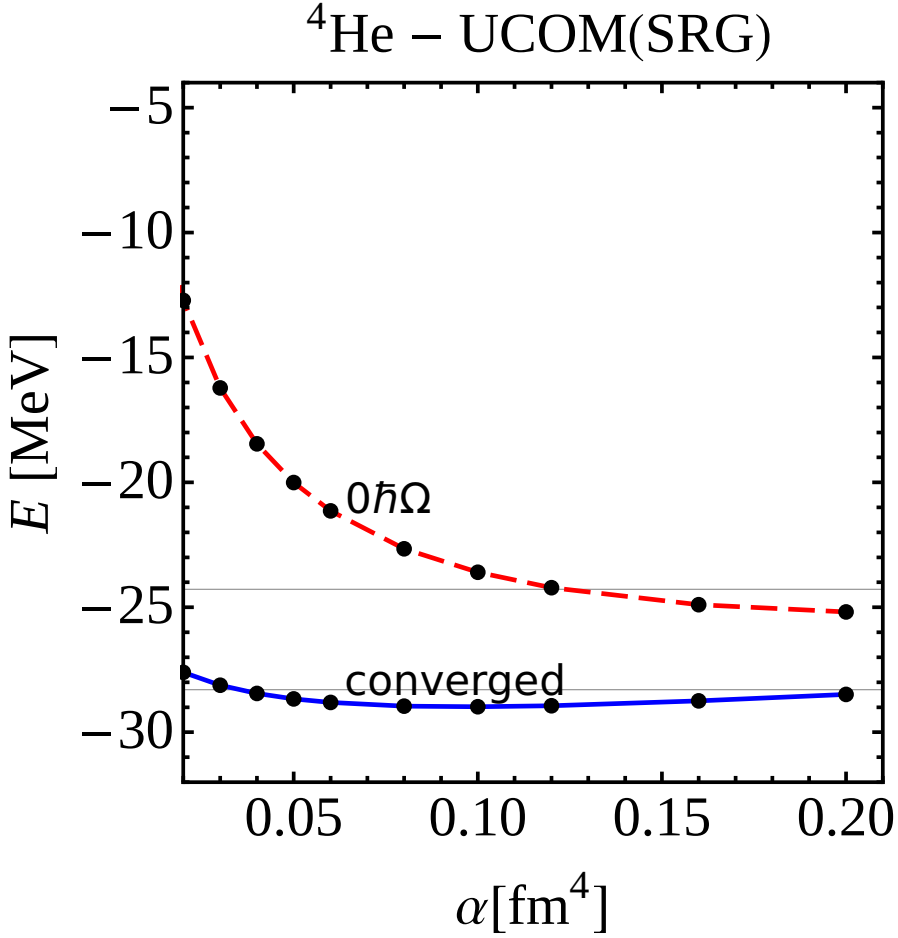

- convergence much improved compared to bare interaction
- effective interaction – in two-body approximation – converges to different energy then bare interaction
- transformed interaction can be tuned to obtain simultaneously (almost) exact ^{3}He and ^{4}He binding energies

UCOM(SRG)

NCSM ^{6}Li/^{7}Li ground state energy

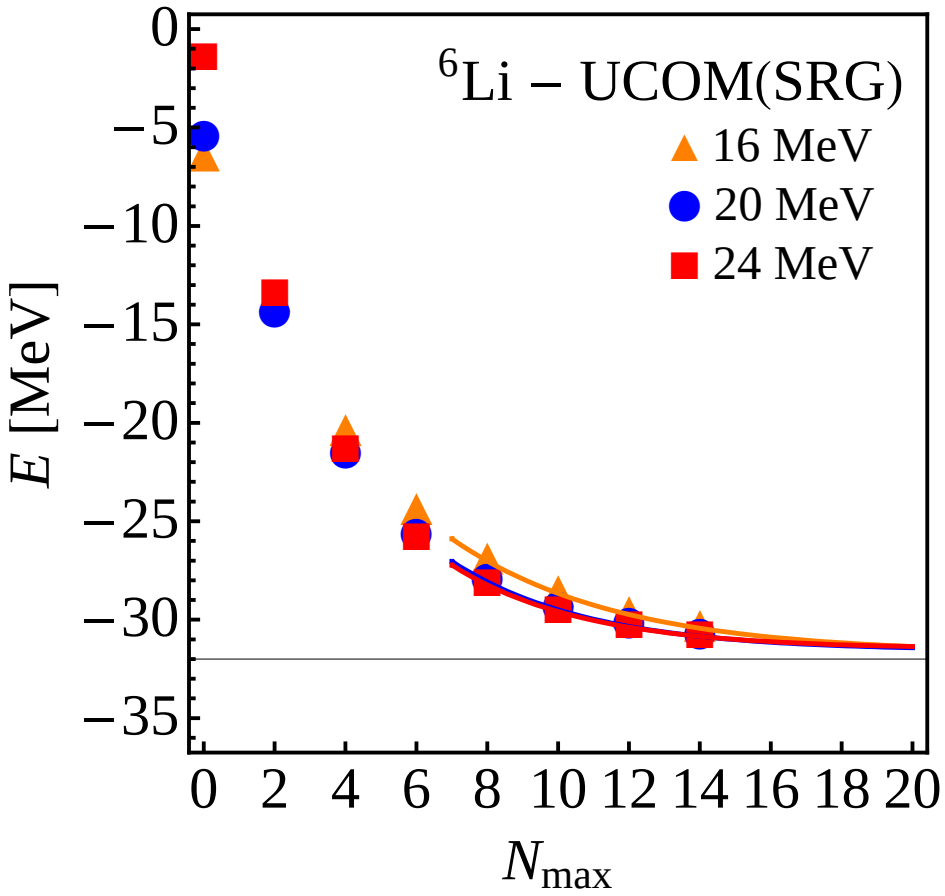

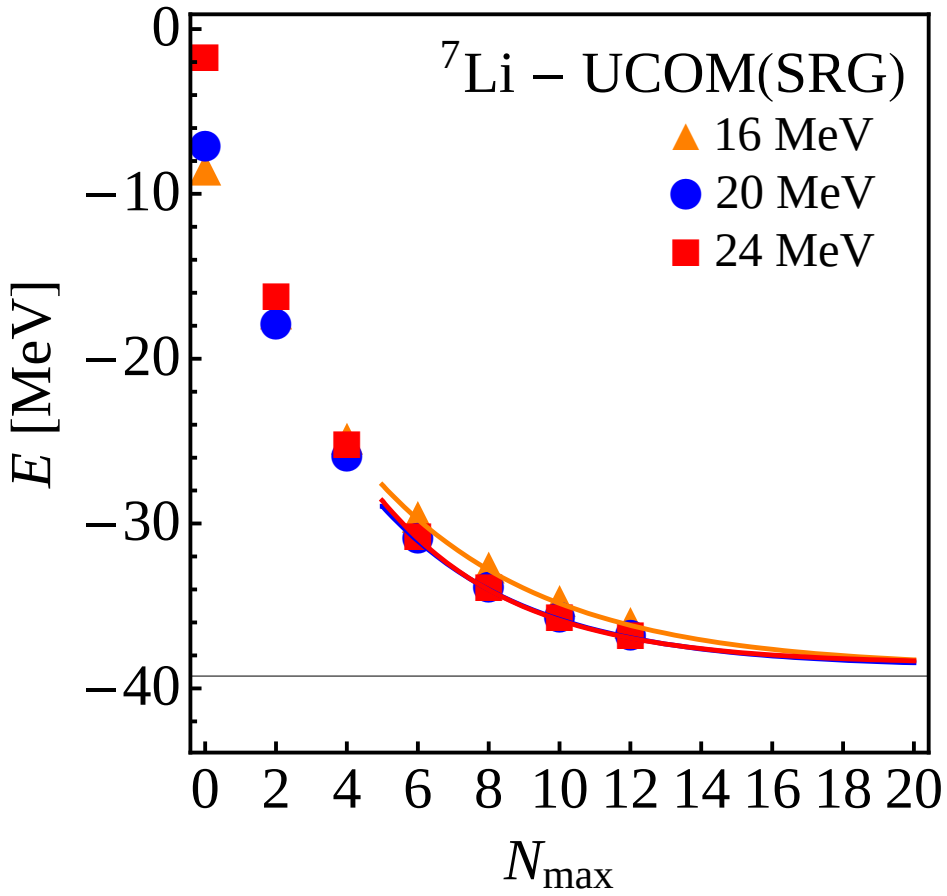

- tuned interaction also works reasonably well for heavier nuclei

NCSM ^{7}Li spectrum

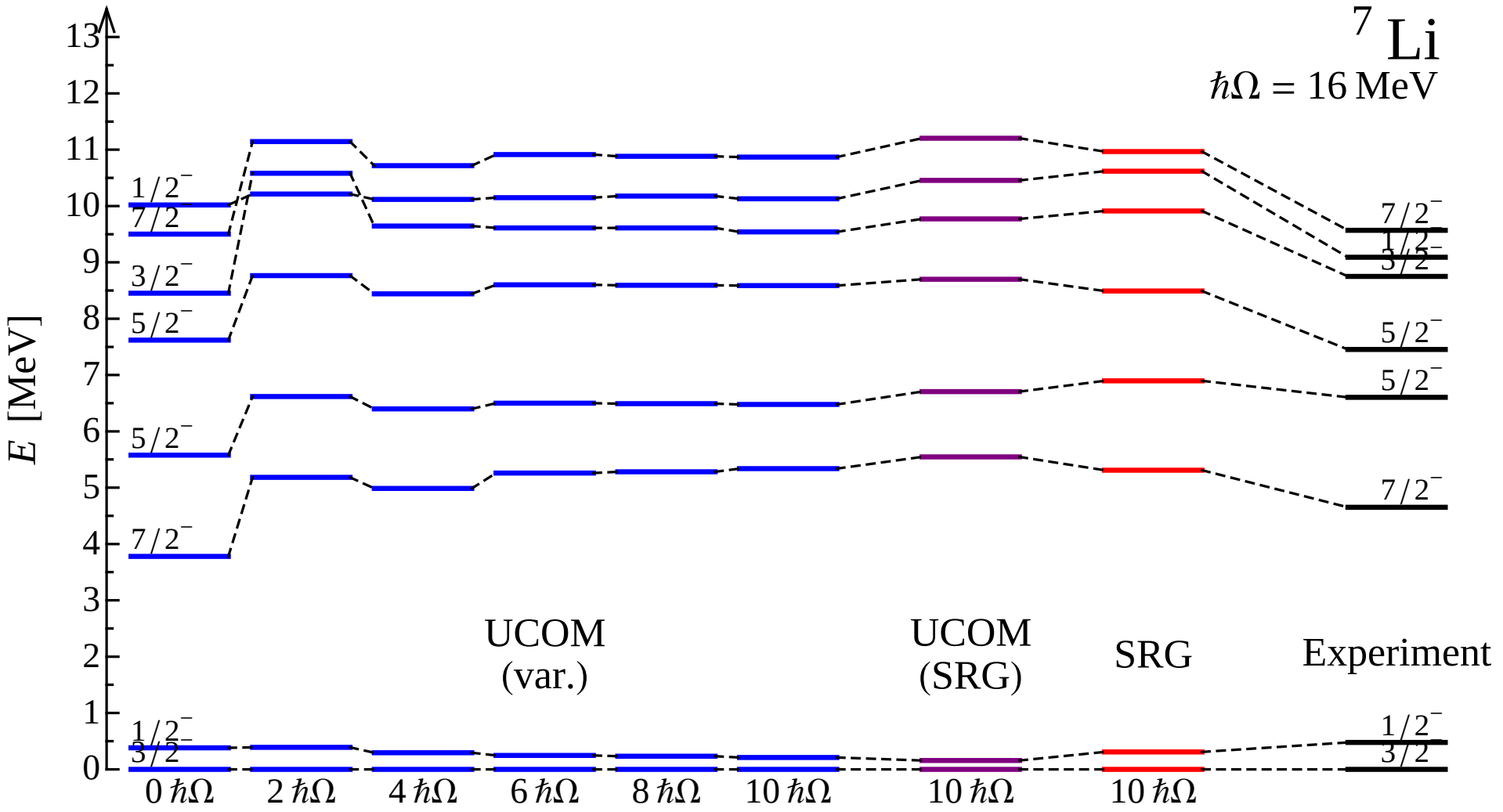

UCOM(SRG)

NCSM ^{6}Li/^{7}Li radii

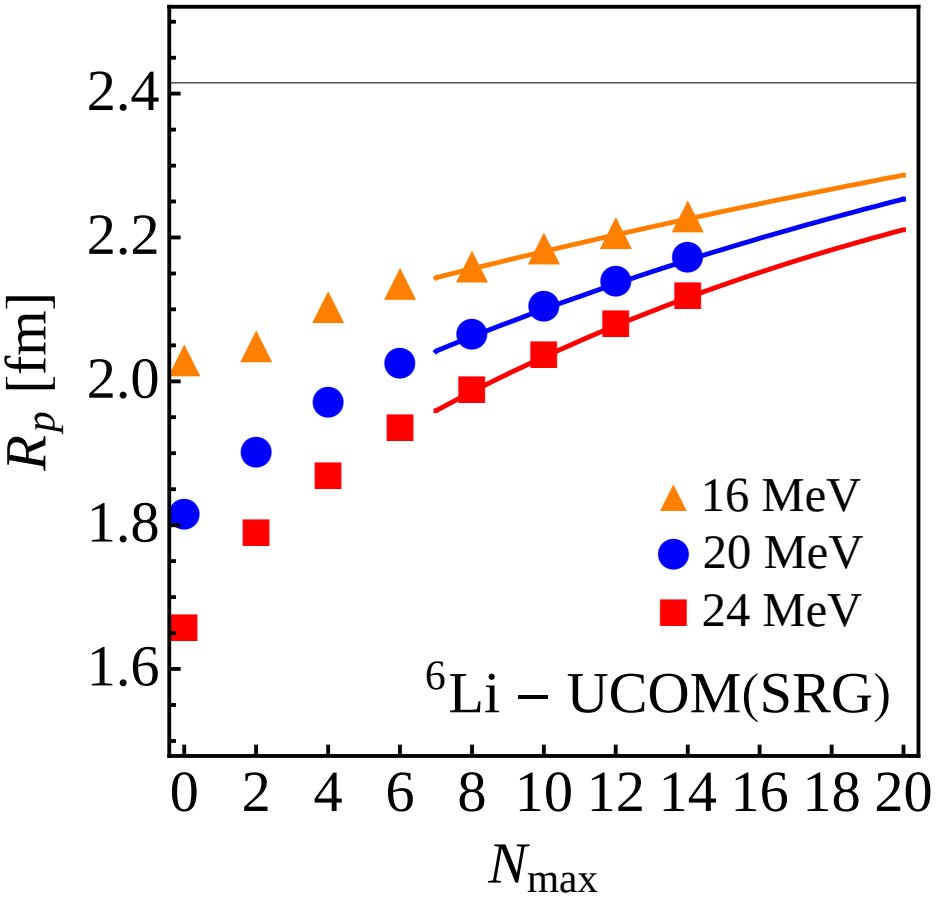

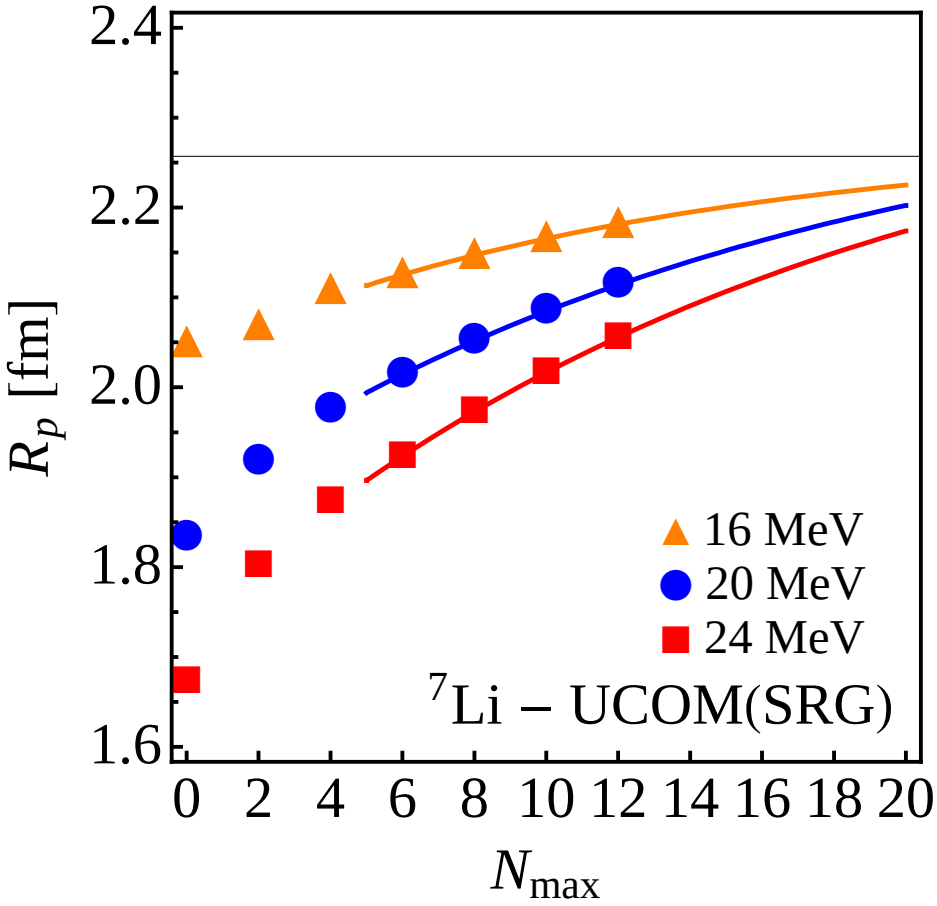

- radii converge worse than energies
- harmonic oscillator basis not well suited to describe tails of weakly bound nuclei

Halos, Clusters, . . .

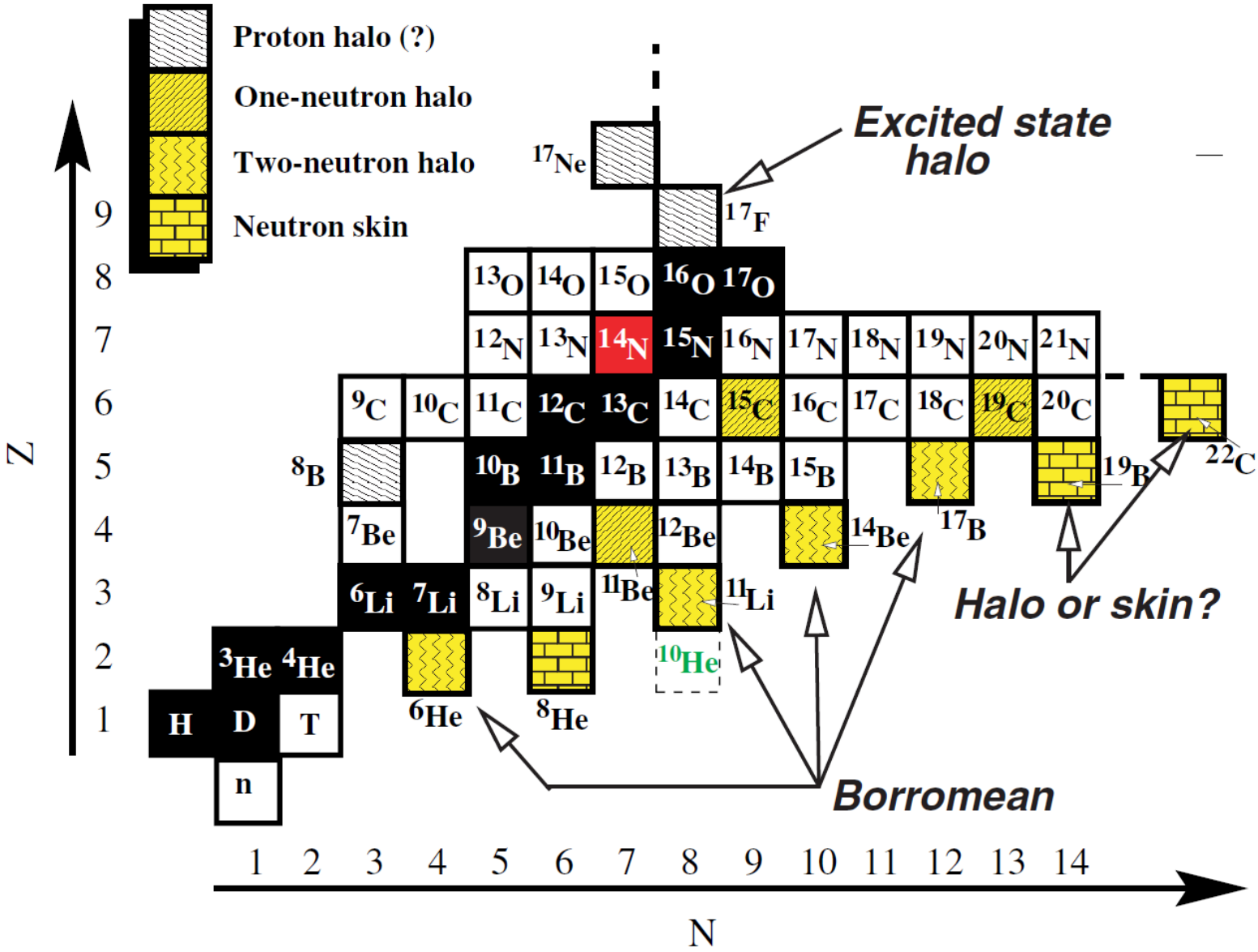

Al-Khalili, Nunes, J. Phys. G **29**, R89 (2003)

Fermionic Molecular Dynamics

Fermionic

Slater determinant

$$\left| Q \right\rangle = \underset{\sim}{\mathcal{A}} \left(\left| q_1 \right\rangle \otimes \cdots \otimes \left| q_A \right\rangle \right)$$

- antisymmetrized A-body state

Feldmeier, Schnack, Rev. Mod. Phys. **72** (2000) 655

Neff, Feldmeier, Nucl. Phys. **A738** (2004) 357

Fermionic Molecular Dynamics

Fermionic

Slater determinant

$$\left| Q \right\rangle = \underset{\sim}{\mathcal{A}} \left(\left| q_1 \right\rangle \otimes \cdots \otimes \left| q_A \right\rangle \right)$$

- antisymmetrized A-body state

Molecular

single-particle states

$$\left\langle \mathbf{x} \middle| q \right\rangle = \exp\left\{ -\frac{(\mathbf{x} - \mathbf{b})^2}{2a} \right\} \otimes \left| \chi^{\uparrow}, \chi^{\downarrow} \right\rangle \otimes \left| \xi \right\rangle$$

- Gaussian wave-packets in phase-space (complex parameter **b** encodes mean position and mean momentum), spin is free, isospin is fixed
- width a is an independent variational parameter for each wave packet
- use one or two wave packets for each single particle state

Feldmeier, Schnack, Rev. Mod. Phys. **72** (2000) 655

Neff, Feldmeier, Nucl. Phys. **A738** (2004) 357

FMD
Fermionic Molecular Dynamics

Fermionic

Slater determinant

$$\left| Q \right\rangle = \underset{\sim}{\mathcal{A}} \left(\left| q_1 \right\rangle \otimes \cdots \otimes \left| q_A \right\rangle \right)$$

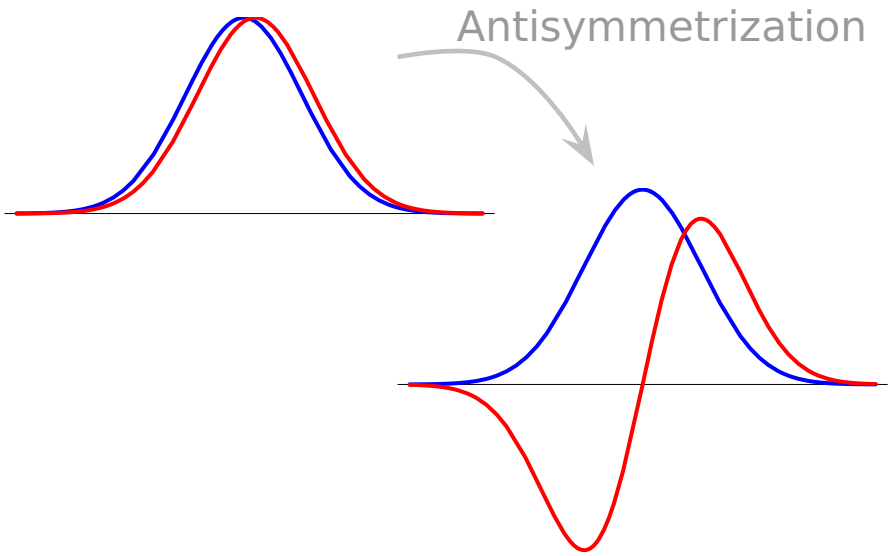

- antisymmetrized A-body state

Molecular

single-particle states

$$\left\langle \mathbf{x} \middle| q \right\rangle = \exp\left\{ -\frac{(\mathbf{x}-\mathbf{b})^2}{2a} \right\} \otimes \left| \chi^{\uparrow}, \chi^{\downarrow} \right\rangle \otimes \left| \xi \right\rangle$$

- Gaussian wave-packets in phase-space (complex parameter **b** encodes mean position and mean momentum), spin is free, isospin is fixed
- width a is an independent variational parameter for each wave packet
- use one or two wave packets for each single particle state

Feldmeier, Schnack, Rev. Mod. Phys. **72** (2000) 655

Neff, Feldmeier, Nucl. Phys. **A738** (2004) 357

FMD

Fermionic Molecular Dynamics

Fermionic

Slater determinant

$$|Q\rangle = \mathcal{A}\left(|q_1\rangle \otimes \cdots \otimes |q_A\rangle\right)$$

- antisymmetrized A-body state

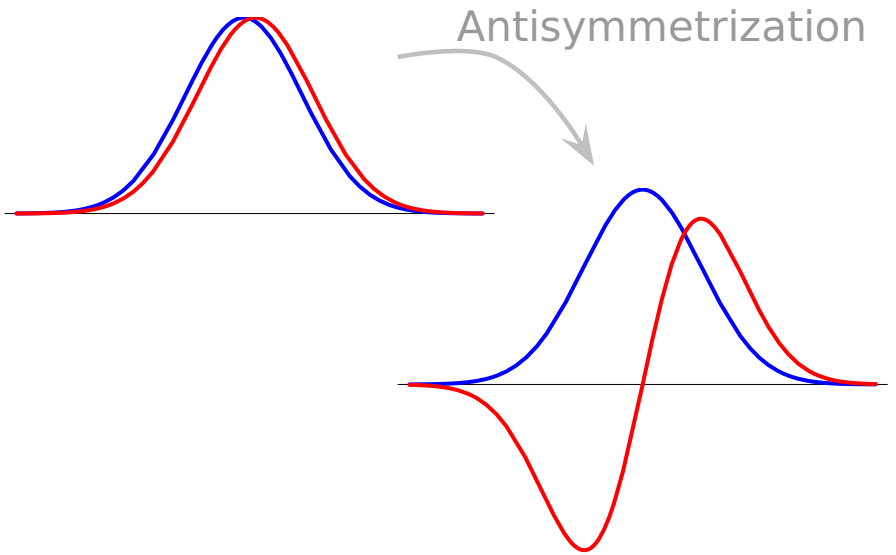

Molecular

single-particle states

$$\langle \mathbf{x}|q\rangle = \exp\left\{-\frac{(\mathbf{x}-\mathbf{b})^2}{2a}\right\} \otimes |\chi^{\uparrow},\chi^{\downarrow}\rangle \otimes |\xi\rangle$$

- Gaussian wave-packets in phase-space (complex parameter **b** encodes mean position and mean momentum), spin is free, isospin is fixed
- width a is an independent variational parameter for each wave packet
- use one or two wave packets for each single particle state

see also
Antisymmetrized Molecular Dynamics
Horiuchi, Kanada-En'yo, Kimura, . . .

Feldmeier, Schnack, Rev. Mod. Phys. **72** (2000) 655

Neff, Feldmeier, Nucl. Phys. **A738** (2004) 357

Interaction Matrix Elements

(One-body) Kinetic Energy

$$\langle q_k \left| \underset{\sim}{T} \right| q_l \rangle = \langle a_k \mathbf{b}_k \left| \underset{\sim}{T} \right| a_l \mathbf{b}_l \rangle \langle \chi_k | \chi_l \rangle \langle \xi_k | \xi_l \rangle$$

$$\langle a_k \mathbf{b}_k \left| \underset{\sim}{T} \right| a_l \mathbf{b}_l \rangle = \frac{1}{2m} \left(\frac{3}{a_k^\star + a_l} - \frac{(\mathbf{b}_k^\star - \mathbf{b}_l)^2}{(a_k^\star + a_l)^2} \right) R_{kl}$$

(Two-body) Potential

- fit radial dependencies by (a sum of) Gaussians

$$G(\mathbf{x}_1 - \mathbf{x}_2) = \exp\left\{ -\frac{(\mathbf{x}_1 - \mathbf{x}_2)^2}{2\kappa} \right\}$$

- Gaussian integrals

$$\alpha_{klmn} = \frac{a_k{}^\star a_m}{a_k{}^\star + a_m} + \frac{a_l{}^\star a_n}{a_l{}^\star + a_n}$$

$$\boldsymbol{\rho}_{klmn} = \frac{a_m \mathbf{b}_k{}^\star + a_k{}^\star \mathbf{b}_m}{a_k{}^\star + a_m} - \frac{a_n \mathbf{b}_l{}^\star + a_l{}^\star \mathbf{b}}{a_l{}^\star + a_n}$$

$$R_{km} = \langle a_k \mathbf{b}_k \left| a_m \mathbf{b}_m \right. \rangle$$

$$\langle a_k \mathbf{b}_k, a_l \mathbf{b}_l \left| \underset{\sim}{G} \right| a_m \mathbf{b}_m, a_n \mathbf{b}_n \rangle = R_{km} R_{ln} \left(\frac{\kappa}{\alpha_{klmn} + \kappa} \right)^{3/2} \exp\left\{ -\frac{\boldsymbol{\rho}_{klmn}^2}{2(\alpha_{klmn} + \kappa)} \right\}$$

- analytical formulas for matrix elements

Operator Representation of V_{UCOM}

$$\underset{\sim}{C}^{\dagger}(\underset{\sim}{T}+\underset{\sim}{V})\underset{\sim}{C} \;=\; \underset{\sim}{T}$$

one-body kinetic energy

$$+\sum_{ST}\hat{V}_{c}^{ST}(r)+\frac{1}{2}(\underset{\sim}{p_r}^2\,\hat{V}_{p^2}^{ST}(r)+\hat{V}_{p^2}^{ST}(r)\,\underset{\sim}{p_r}^2)+\hat{V}_{l^2}^{ST}(r)\,\underset{\sim}{\mathbf{l}}^2$$

central potentials

$$+\sum_{T}\hat{V}_{ls}^{T}(r)\,\underset{\sim}{\mathbf{l}}\cdot\underset{\sim}{\mathbf{s}}+\hat{V}_{l^2ls}^{T}(r)\,\underset{\sim}{\mathbf{l}}^2\underset{\sim}{\mathbf{l}}\cdot\underset{\sim}{\mathbf{s}}$$

spin-orbit potentials

$$+\sum_{T}\hat{V}_{t}^{T}(r)\,\underset{\sim}{S}_{12}(\mathbf{r},\mathbf{r})+\hat{V}_{trp_\Omega}^{T}(r)\,\underset{\sim}{p_r}\,\underset{\sim}{S}_{12}(\mathbf{r},\mathbf{p_\Omega})+\hat{V}_{tll}^{T}(r)\,\underset{\sim}{S}_{12}(\mathbf{l},\mathbf{l})+$$
$$\hat{V}_{tp_\Omega p_\Omega}^{T}(r)\,\underset{\sim}{S}_{12}(\mathbf{p_\Omega},\mathbf{p_\Omega})+\hat{V}_{l^2tp_\Omega p_\Omega}^{T}(r)\,\underset{\sim}{\mathbf{l}}^2\underset{\sim}{S}_{12}(\mathbf{p_\Omega},\mathbf{p_\Omega})$$

tensor potentials

bulk of tensor force mapped onto central part of correlated interaction

tensor correlations also change the spin-orbit part of the interaction

Nucl. Phys. **A745** (2004) 3

Mean-Field Calculations

Minimization

- minimize Hamiltonian expectation value with respect to all single-particle parameters q_k

$$\min_{\{q_k\}} \frac{\langle Q \left| \underset{\sim}{H} - \underset{\sim}{T}_{cm} \right| Q \rangle}{\langle Q \left| Q \right\rangle}$$

- this is a Hartree-Fock calculation in our particular single-particle basis
- the mean-field may break the symmetries of the Hamiltonian

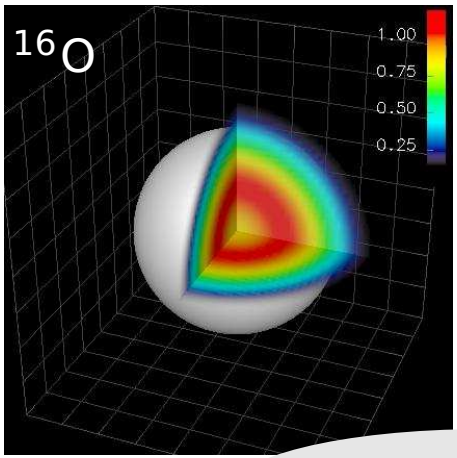

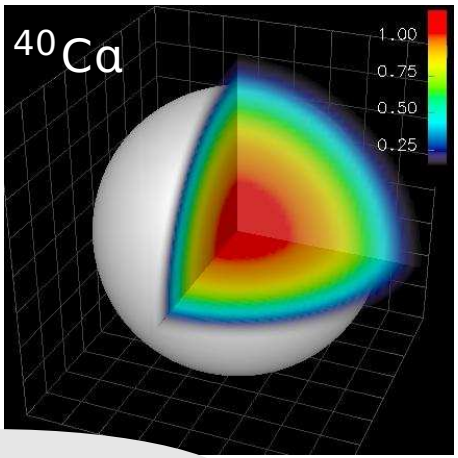

spherical nuclei

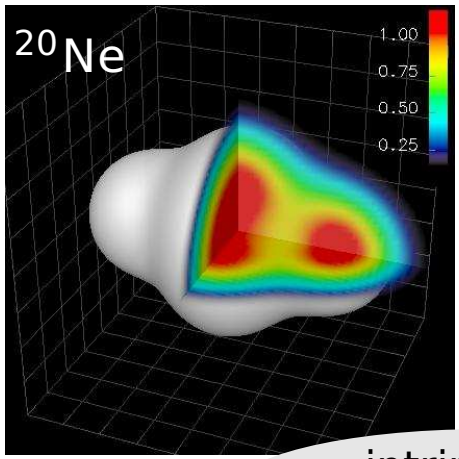

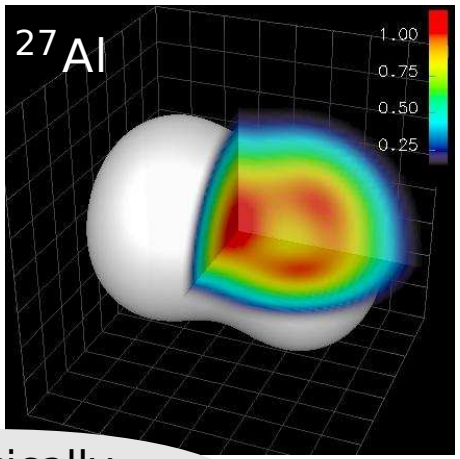

intrinsically deformed nuclei

Projection and Multiconfiguration Mixing

Projection

- Slater determinant may break symmetries of Hamiltonian
- restore symmetries by projection on parity, linear and angular momentum

$$\underset{\sim}{P}^{\pi} = \frac{1}{2}(1 + \pi \underset{\sim}{\Pi})$$

$$\underset{\sim}{P}^{J}_{MK} = \frac{2J+1}{8\pi^2} \int \mathrm{d}^3\Omega \, {D^{J}_{MK}}^{\star}(\Omega) \, \underset{\sim}{R}(\Omega)$$

$$\underset{\sim}{P}^{\mathbf{P}} = \frac{1}{(2\pi)^3} \int \mathrm{d}^3X \; \exp\{-i(\underset{\sim}{\mathbf{P}} - \mathbf{P})\cdot\mathbf{X}\}$$

Projection and Multiconfiguration Mixing

Projection

- Slater determinant may break symmetries of Hamiltonian
- restore symmetries by projection on parity, linear and angular momentum

$$\underset{\sim}{P}^{\pi} = \frac{1}{2}(1 + \pi \underset{\sim}{\Pi})$$

$$\underset{\sim}{P}^{J}_{MK} = \frac{2J+1}{8\pi^2} \int \mathrm{d}^3\Omega \, D^{J}_{MK}{}^{\star}(\Omega) \, \underset{\sim}{R}(\Omega)$$

Creating Basis States

- full **Variation after Angular Momentum and Parity Projection** (VAP) for spins of lowest states
- constrain radius, dipole, quadrupole or octupole moments to generate additonal basis states
- For heavier nuclei (*sd*-shell) only Projection after Variation possible

$$\underset{\sim}{P}^{\mathbf{P}} = \frac{1}{(2\pi)^3} \int \mathrm{d}^3X \, \exp\{-i(\underset{\sim}{\mathbf{P}} - \mathbf{P})\cdot\mathbf{X}\}$$

Projection and Multiconfiguration Mixing

Projection

- Slater determinant may break symmetries of Hamiltonian
- restore symmetries by projection on parity, linear and angular momentum

$$\underset{\sim}{P}^{\pi} = \frac{1}{2}(1 + \pi \underset{\sim}{\Pi})$$

$$\underset{\sim}{P}^{J}_{MK} = \frac{2J+1}{8\pi^2} \int \mathrm{d}^3\Omega \, D^{J}_{MK}{}^{\star}(\Omega) \, \underset{\sim}{R}(\Omega)$$

Creating Basis States

- full **Variation after Angular Momentum and Parity Projection** (VAP) for spins of lowest states
- constrain radius, dipole, quadrupole or octupole moments to generate additonal basis states
- For heavier nuclei (*sd*-shell) only Projection after Variation possible

$$\underset{\sim}{P}^{\mathbf{P}} = \frac{1}{(2\pi)^3} \int \mathrm{d}^3X \, \exp\{-i(\underset{\sim}{\mathbf{P}} - \mathbf{P})\cdot\mathbf{X}\}$$

Multiconfiguration Mixing Calculations

- **diagonalize** Hamiltonian in set of projected intrinsic states

$$\left\{ \left| Q^{(\alpha)} \right\rangle, \quad \alpha = 1, \ldots, N \right\}$$

$$\sum_{K'b} \left\langle Q^{(a)} \right| \underset{\sim}{H} \underset{\sim}{P}^{J^{\pi}}_{KK'} \underset{\sim}{P}^{\mathbf{P}=0} \left| Q^{(b)} \right\rangle \cdot c^{\alpha}_{K'b} =$$

$$E^{J^{\pi}\alpha} \sum_{K'b} \left\langle Q^{(a)} \right| \underset{\sim}{P}^{J^{\pi}}_{KK'} \underset{\sim}{P}^{\mathbf{P}=0} \left| Q^{(b)} \right\rangle \cdot c^{\alpha}_{K'b}$$

PAV and VAP

^{4}He-^{4}He

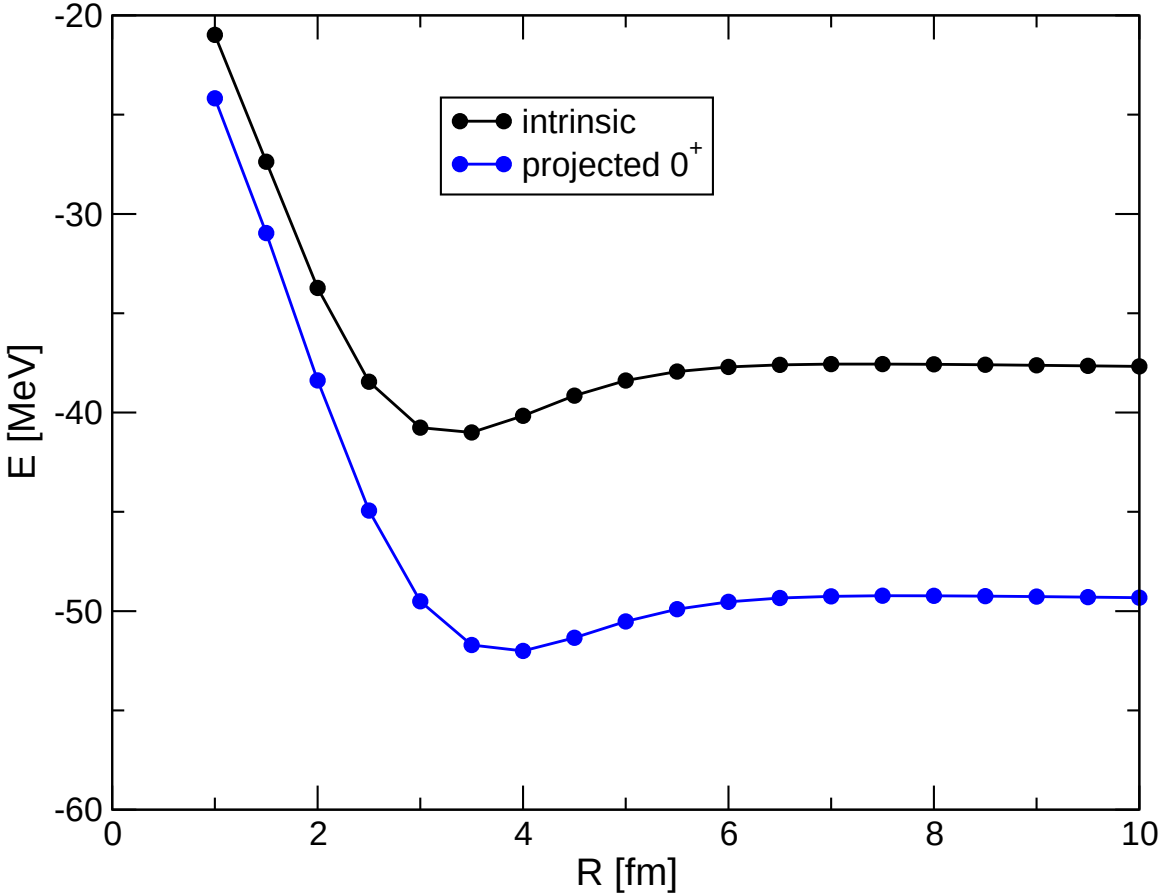

^{4}He-^{4}He-^{4}He

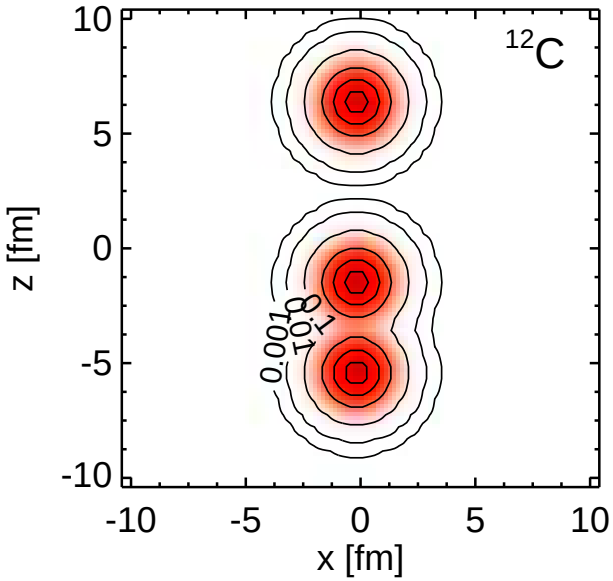

E_{intr} = -49.39 MeV
E_{proj} = -61.31 MeV

- angular momentum projection lowers kinetic energy by delocalizing clusters
- correlation energies can be very significant

^{3}He(α,γ)^{7}Be radiative capture

one of the key reactions in the solar pp-chains

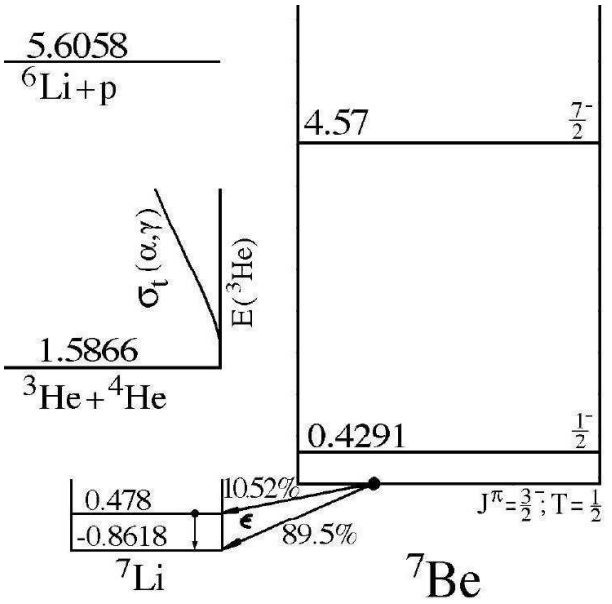

Effective Nucleon-Nucleon interaction:

UCOM(SRG) $\alpha = 0.20$ **fm**^{4} **–** $\lambda \approx 1.5$ **fm**$^{-1}$

Many-Body Approach:

Fermionic Molecular Dynamics

- **Internal region: VAP configurations with radius constraint**
- **External region: Brink-type cluster configurations**
- **Matching to Coulomb solutions: Microscopic** R**-matrix method**

Results:

- ^{7}Be **bound and scattering states**
- **Astrophysical** S**-factor**

Theoretical Approaches

Potential models (Kim *et al.* 1982, Mohr 2009, . . .)

- ^{4}He and ^{3}He are considered as point-like particles
- interacting via an effective nucleus-nucleus potential fitted to bound state properties and phase shifts
- ANCs calculated from *ab initio* wave functions (Nollett 2001, Navratil *et al.* 2007)

Microscopic Cluster Model (Tang *et al.* 1981, Langanke 1986, Kajino 1986 . . .)

- antisymmetrized wave function built with ^{4}He and ^{3}He clusters
- some attempts to include polarization effects by adding other channels like ^{6}Li plus proton
- interacting via an effective nucleon-nucleon potential, adjusted to describe bound state properties and phase shifts

Our Aim

- fully microscopic wave functions with cluster configurations at large distances and additional polarized A-body configurations in the interaction region
- using a realistic effective interaction

FMD model space

Frozen configurations

- antisymmetrized wave function built with ^{4}He and ^{3}He FMD clusters up to channel radius a=12 fm

Polarized configurations

- FMD wave functions obtained by VAP on $1/2^-$, $3/2^-$, $5/2^-$, $7/2^-$ and $1/2^+$, $3/2^+$ and $5/2^+$ combined with radius constraint in the interaction region

Boundary conditions

- Match relative motion of clusters at channel radius to Whittaker/Coulomb functions with the **microscopic *R*-matrix** method of the Brussels group

  D. Baye, P.-H. Heenen, P. Descouvemont

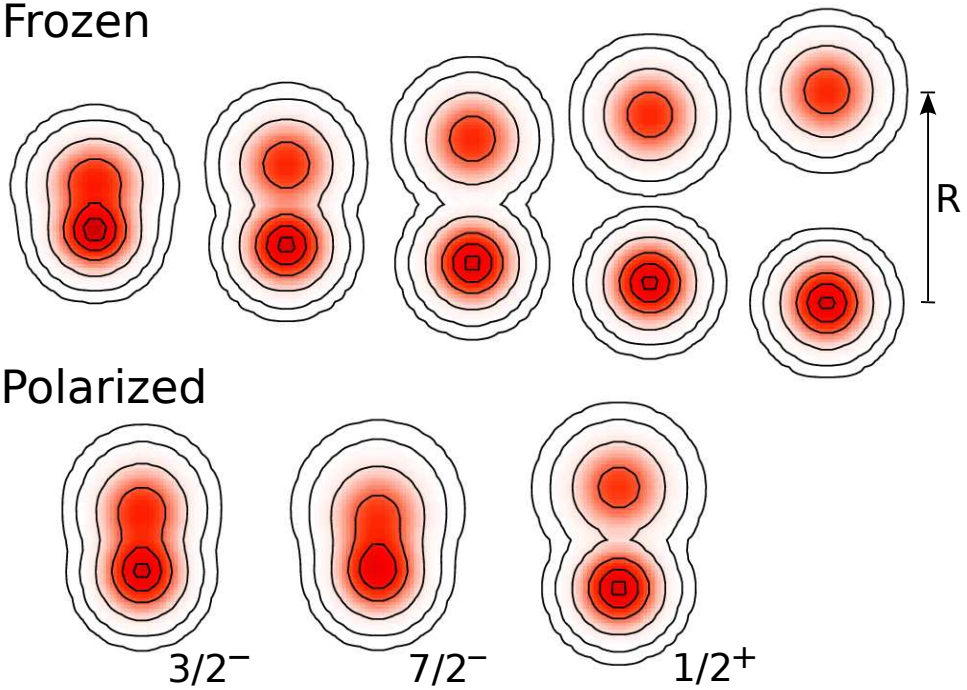

Slater determinants and RGM wave functions

- Divide model space into internal and external region at channel radius a
- In internal region wave function is described microscopically with FMD Slater determinants
- In external region wave function is considered as a system of two point-like clusters
- (Microscopic) cluster wave function – Slater determinant

$$\left| Q^{ab}(\mathbf{R}) \right\rangle = \frac{1}{\sqrt{c_{ab}}} \mathcal{A} \left\{ \left| Q^{a}(-\frac{m_b}{m_a+m_b}\mathbf{R}) \right\rangle \otimes \left| Q^{b}(\frac{m_a}{m_a+m_b}\mathbf{R}) \right\rangle \right\}$$

- Projection on total linear momentum decouples intrinsic motion, relative motion of clusters and total center-of-masss

$$\left| Q^{ab}(\mathbf{R}); \mathbf{P}=0 \right\rangle = \int \mathrm{d}^3 r \, \tilde{\Gamma}(\mathbf{r}-\mathbf{R}) \left| \Phi^{ab}(\mathbf{r}) \right\rangle \otimes \left| \mathbf{P}_{cm}=0 \right\rangle$$

using RGM basis states

$$\left\langle \boldsymbol{\rho}, \xi_a, \xi_b \right| \left. \Phi^{ab}(\mathbf{r}) \right\rangle = \frac{1}{\sqrt{c_{ab}}} \mathcal{A} \left\{ \delta(\boldsymbol{\rho}-\mathbf{r}) \Phi^{a}(\xi_a) \Phi^{b}(\xi_b) \right\}$$

RGM norm kernel

$$n^{ab}(\mathbf{r}, \mathbf{r}') = \left\langle \Phi^{ab}(\mathbf{r}) \right| \left. \Phi^{ab}(\mathbf{r}') \right\rangle$$

Slater determinants and RGM wave functions

- Relative motion in Slater determinant described by Gaussian

$$\tilde{\Gamma}(\mathbf{r}-\mathbf{R}) = \left(\frac{\beta_{\text{rel}}}{\pi^2 a_{\text{rel}}}\right)^{3/4} \exp\left(-\frac{(\mathbf{r}-\mathbf{R})^2}{2a_{\text{rel}}}\right)$$

with

$$a_{\text{rel}} = \frac{a_a A_b + a_b A_a}{A_a A_b}, \quad \beta_{\text{rel}} = \frac{a_a a_b}{a_a A_b + a_b A_a}$$

- Overlap of full wave function with RGM cluster basis

$$\psi(\mathbf{r}) = \int \mathrm{d}^3 r'\, n^{1/2}(\mathbf{r},\mathbf{r}') \langle\, \Phi(\mathbf{r}') \,|\, \Psi \,\rangle$$

- Match asymptotics to Whittaker or Coulomb functions

$$\psi_{\text{b}}(r) = A\,\frac{1}{r} W_{-\eta,L+1/2}(2\kappa r)$$

$$\psi_{\text{scatt}}(r) = \frac{1}{r}\left\{I_L(\eta,kr) - e^{2i\delta} O_L(\eta,kr)\right\}$$

with

$$\kappa = \sqrt{-2\mu E_b}, \quad k = \sqrt{2\mu E}, \quad \eta = \mu \frac{Z_a Z_b e^2}{k}$$

p-wave Bound and Scattering States

Bound states

		Experiment	FMD
^{7}Be	$E_{3/2-}$	-1.59 MeV	-1.49 MeV
	$E_{1/2-}$	-1.15 MeV	-1.31 MeV
	r_{ch}	2.647(17) fm	2.67 fm
	Q	–	-6.83 e fm^2
^{7}Li	$E_{3/2-}$	-2.467 MeV	-2.39 MeV
	$E_{1/2-}$	-1.989 MeV	-2.17 MeV
	r_{ch}	2.444(43) fm	2.46 fm
	Q	-4.00(3) e fm^2	-3.91 e fm^2

- centroid of bound state energies well described if polarized configurations included
- tail of wave functions tested by charge radii and quadrupole moments

Phase shift analysis:

Spiger and Tombrello, PR **163**, 964 (1967)

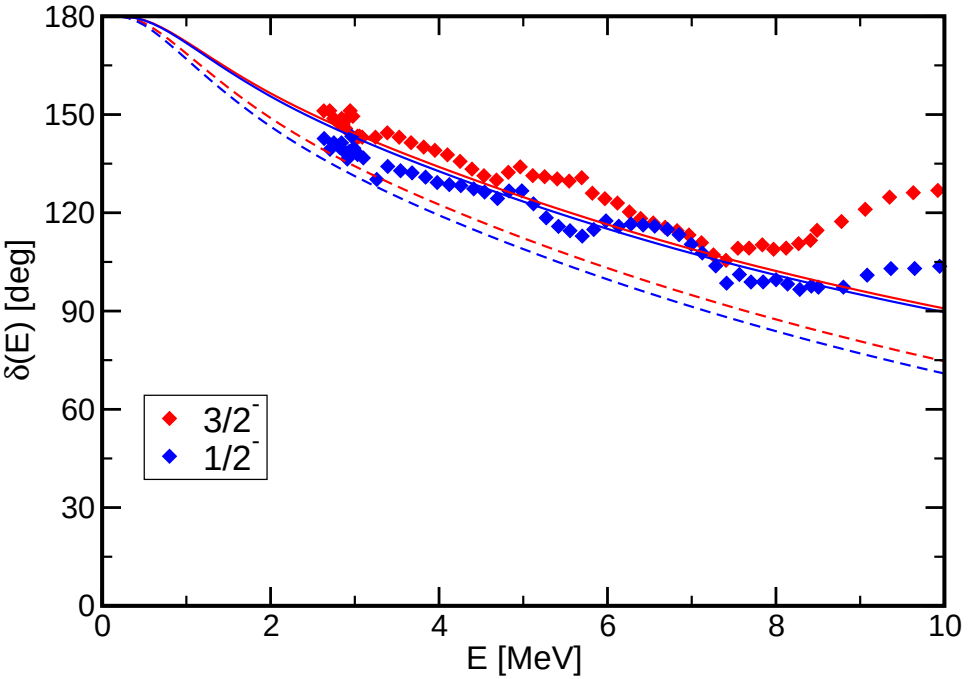

dashed lines – frozen configurations only
solid lines – polarized configurations in interaction region included

- Scattering phase shifts well described, polarization effects important

^{3}He(α,γ)^{7}Be

s-, d- and f-wave Scattering States

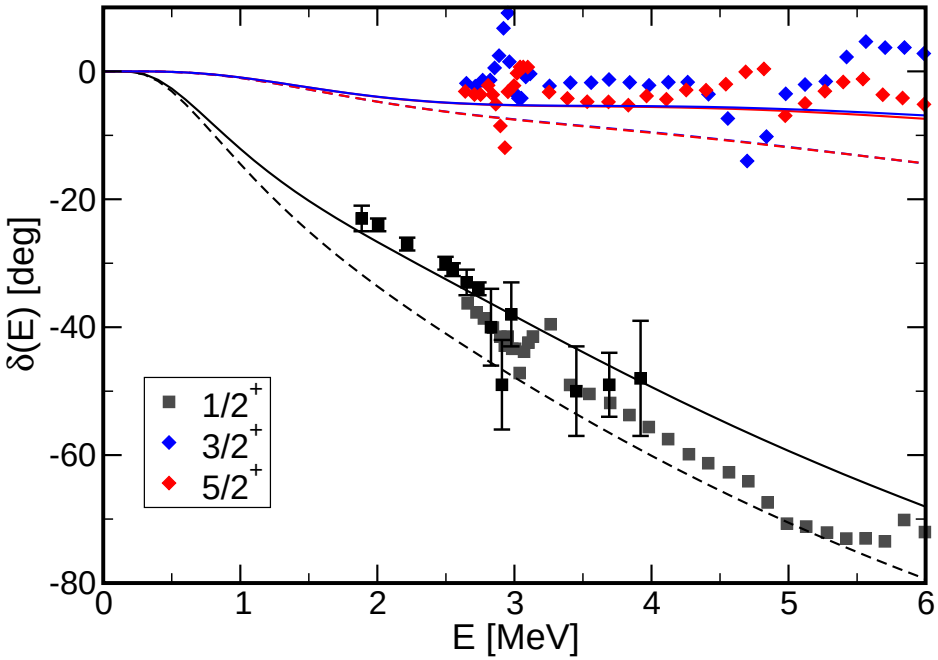

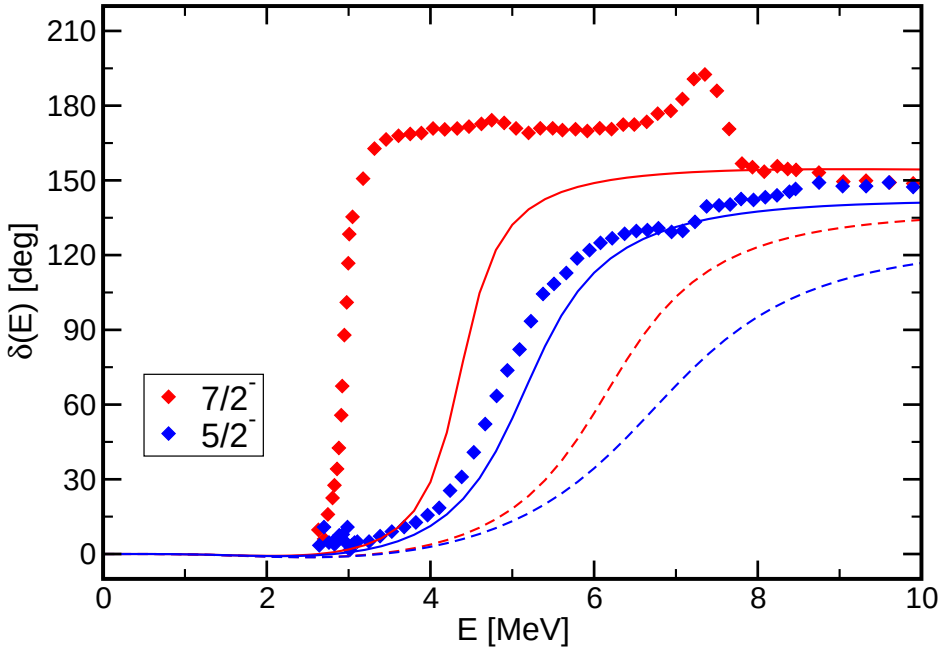

dashed lines – frozen configurations only – solid lines – FMD configurations in interaction region included

- polarization effects important
- s- and d-wave scattering phase shifts well described
- $7/2^-$ resonance too high, $5/2^-$ resonance roughly right, consistent with no-core shell model calculations

$^3\mathrm{He}(\alpha,\gamma)^7\mathrm{Be}$
S-Factor

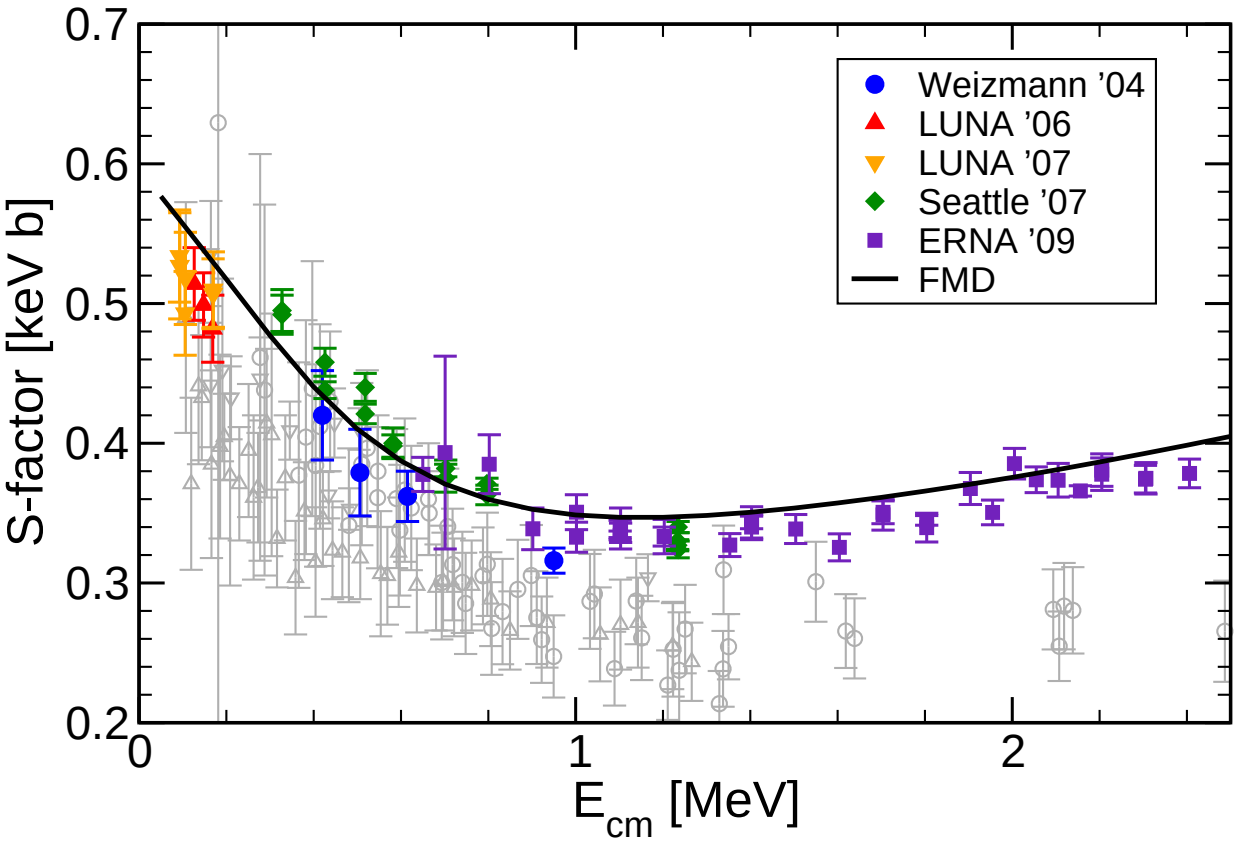

S-factor:

$$S(E) = \sigma(E) E \exp\{2\pi\eta\}$$

$$\eta = \frac{\mu Z_1 Z_2 e^2}{k}$$

Nara Singh *et al.*, PRL **93**, 262503 (2004)
Bemmerer *et al.*, PRL **97**, 122502 (2006)
Confortola *et al.*, PRC **75**, 065803 (2007)
Brown *et al.*, PRC **76**, 055801 (2007)
Di Leva *et al.*, PRL **102**, 232502 (2009)

- dipole transitions from $1/2^+$, $3/2^+$, $5/2^+$ scattering states into $3/2^-$, $1/2^-$ bound states
- ➥ FMD is the only model that describes well the energy dependence and normalization of new high quality data
- ➥ fully microscopic calculation, bound and scattering states are described consistently

^{3}He(α,γ)^{7}Be

Overlap Functions and Dipole Matrixelements

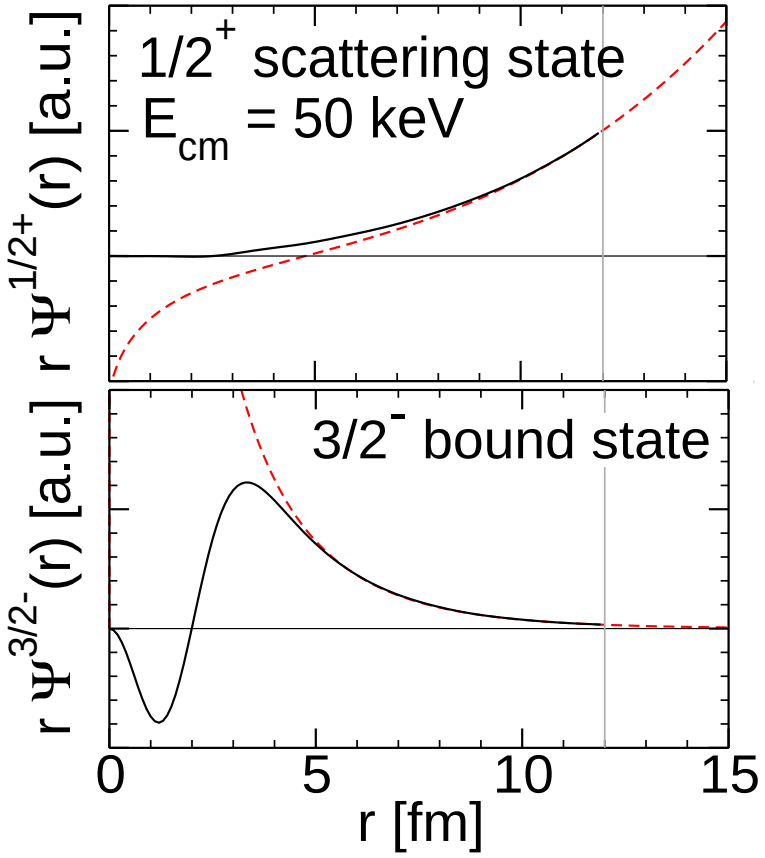

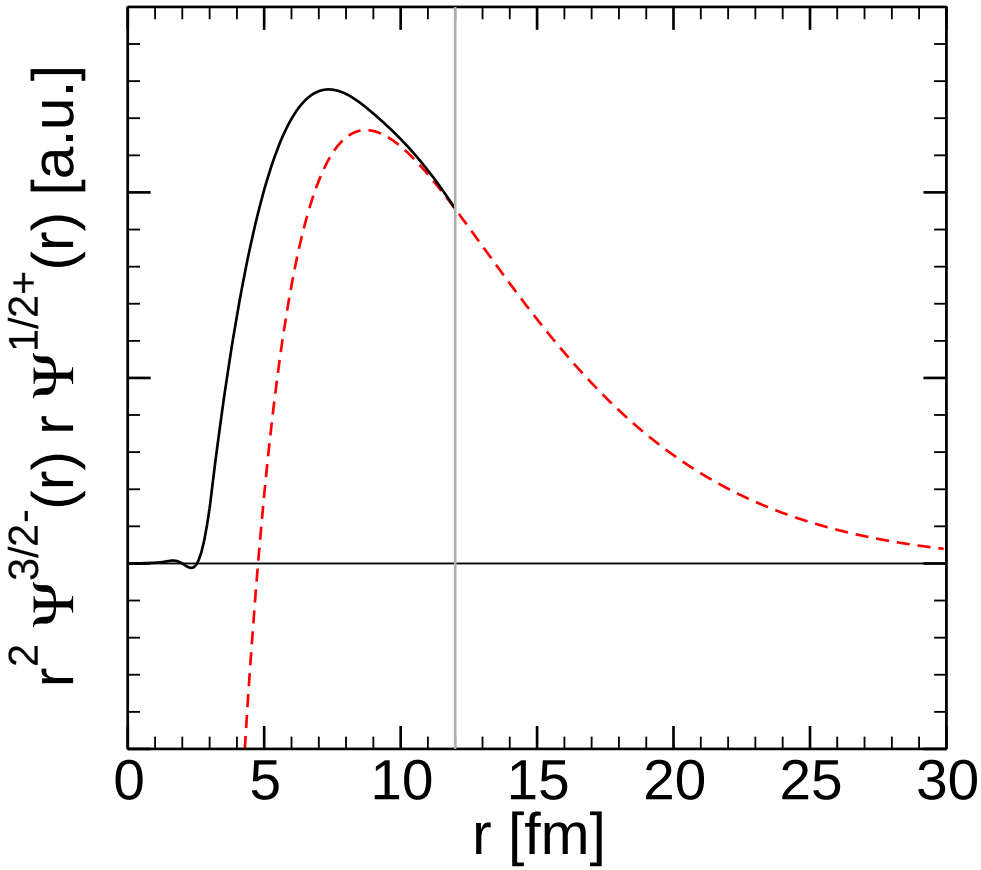

- Overlap functions from projection on RGM-cluster states
- Coulomb and Whittaker functions matched at channel radius a=12 fm
- Dipole matrix elements calculated from overlap functions reproduce full calculation within 2%
- cross section depends significantly on internal part of wave function, description as an “external” capture is too simplified

^{3}He(α,γ)^{7}Be

Energy dependence of the S-Factor

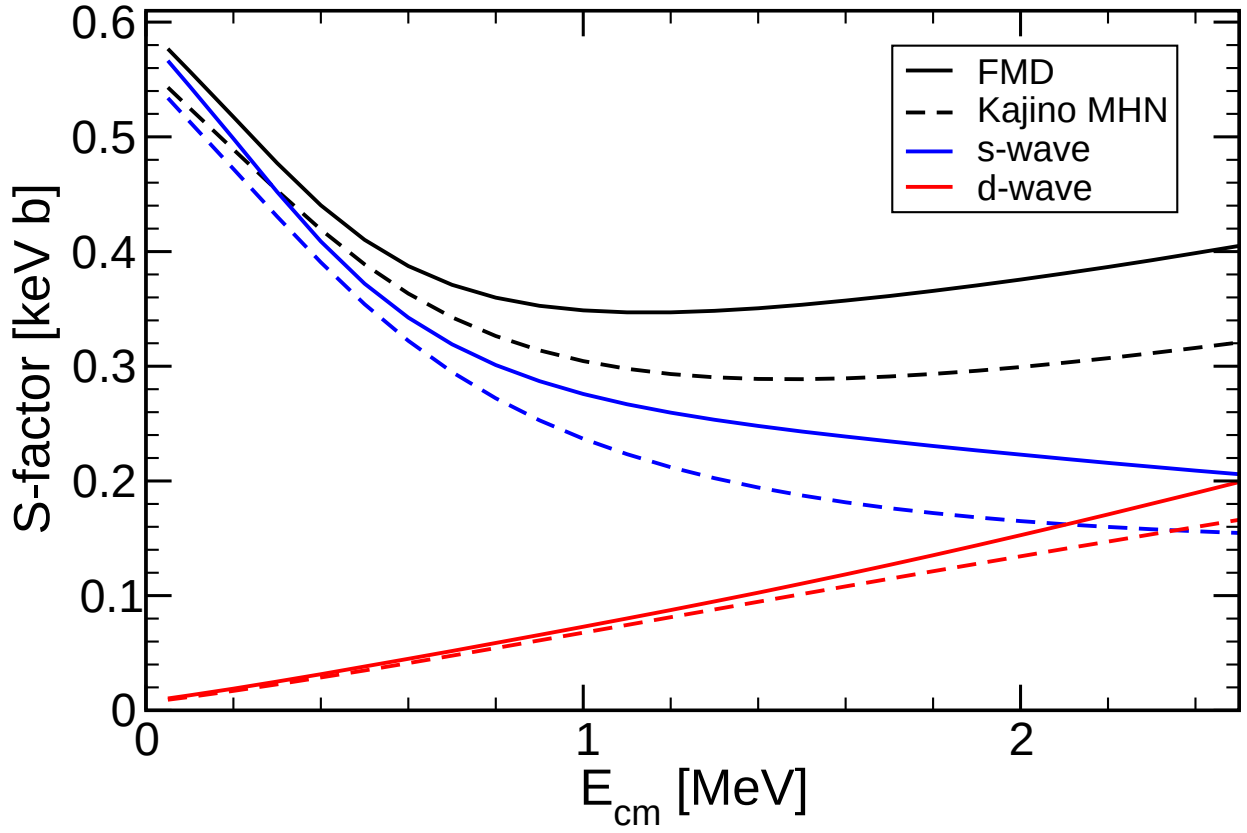

- low-energy *S*-factor dominated by *s*-wave capture
- at 2.5 MeV equal contributions of *s*- and *d*-wave capture
- FMD results differ from Kajino results mainly with respect to *s*-wave capture
- related to short-range part of wave functions ?

$^3H(\alpha,\gamma)^7Li$
S-Factor

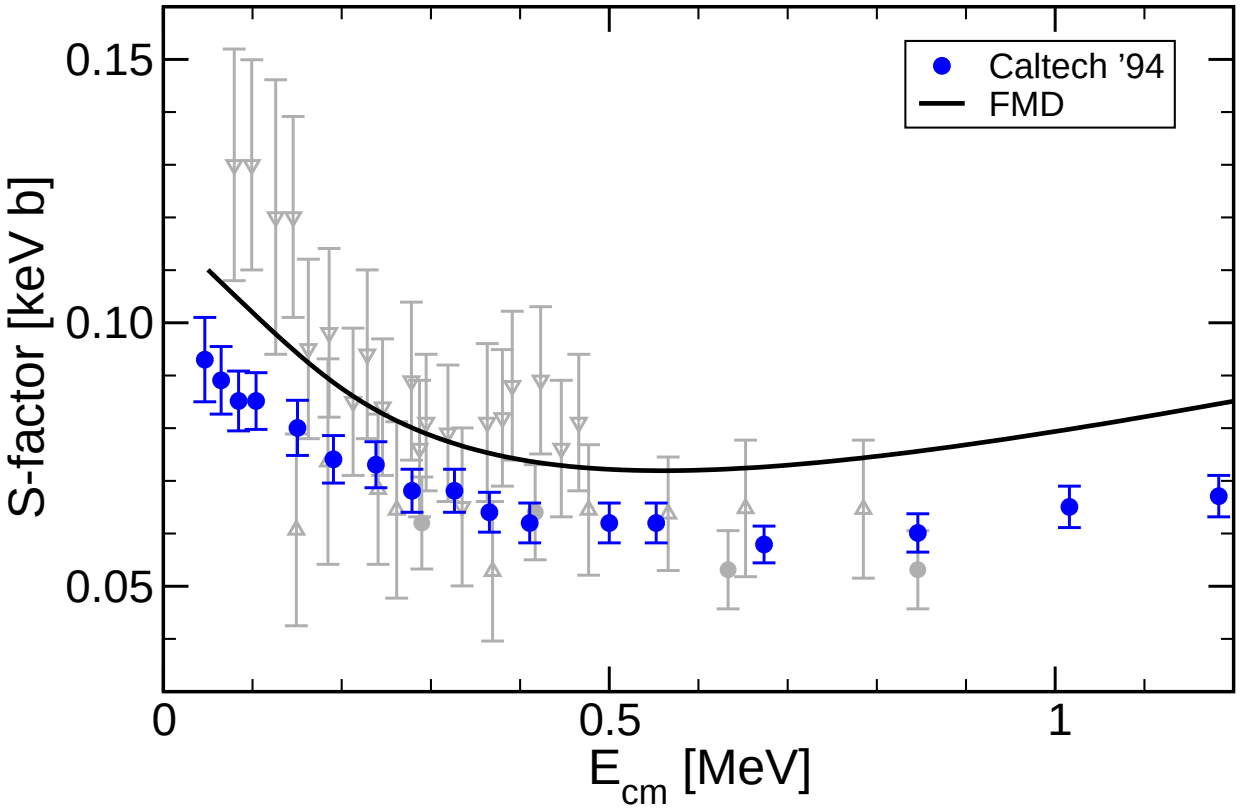

S-factor:

$$S(E) = \sigma(E) E \exp\{2\pi\eta\}$$

$$\eta = \frac{\mu Z_1 Z_2 e^2}{k}$$

Brune *et al.*, PRC **50**, 2205 (1994)

- isospin mirror reaction of $^3He(\alpha,\gamma)^7Be$
- ^7Li bound state properties and phase shifts well described

➨ FMD calculation describes energy dependence of Brune *et al.* data but cross section is larger by about 15%

^{3}He$(\alpha,\gamma)^7$Be and ^{3}H$(\alpha,\gamma)^7$Li
S-Factors consistent ?

^{3}He$(\alpha,\gamma)^7$Be

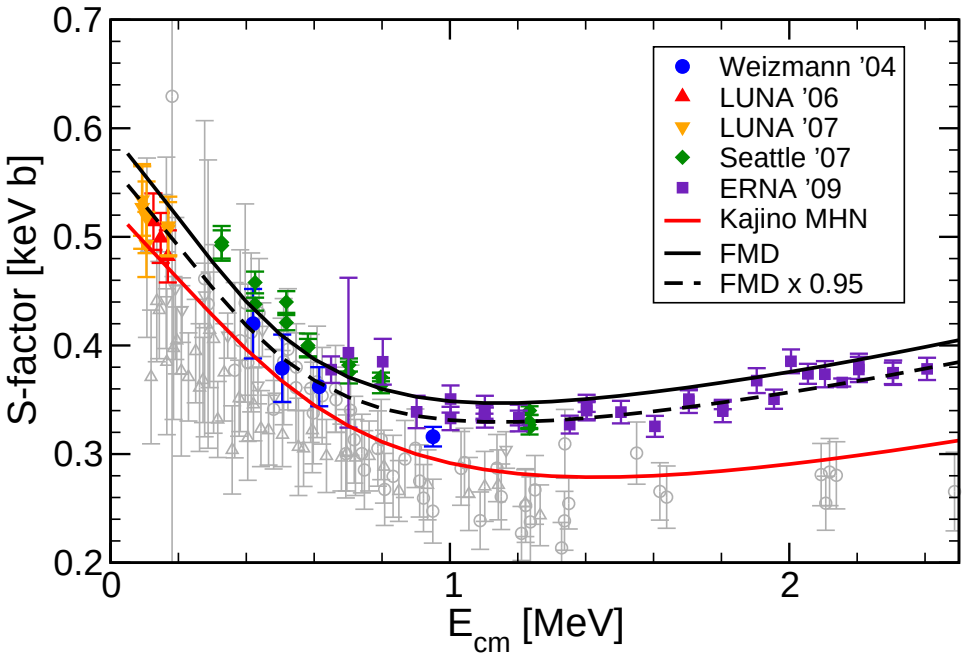

^{3}H$(\alpha,\gamma)^7$Li

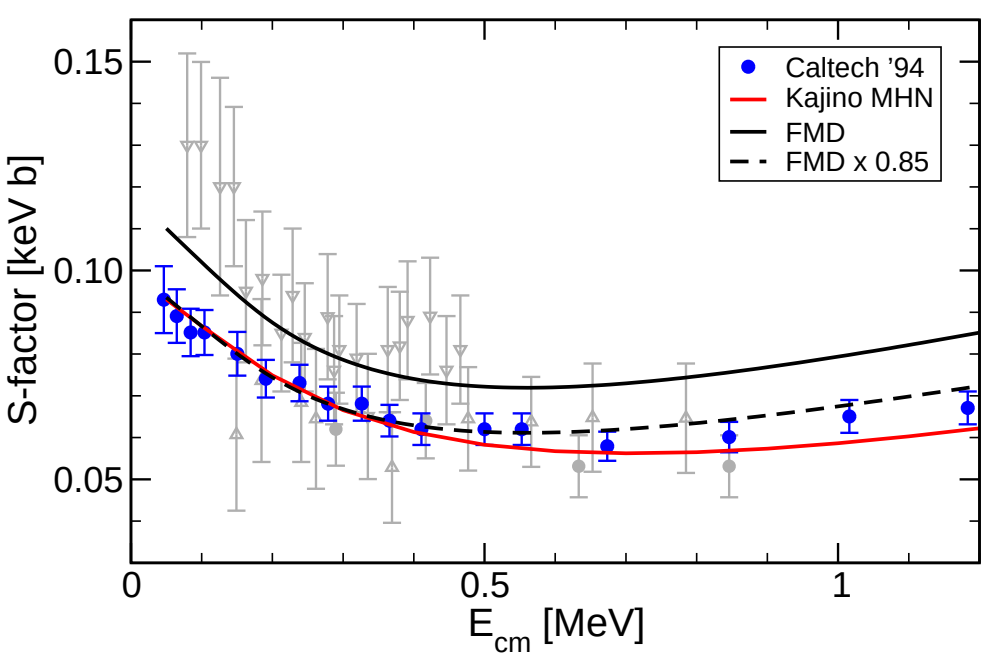

- FMD calculation agrees with normalization and energy dependence of ^{3}He$(\alpha,\gamma)^7$Be data
- FMD calculation agrees with energy dependence but not normalization of ^{3}H$(\alpha,\gamma)^7$Li data
- similar inconsistency observed in other models

^{4}He-n scattering

Phase shift analysis: Bond and Kirk, Nucl. Phys. **A287**, 317 (1977)

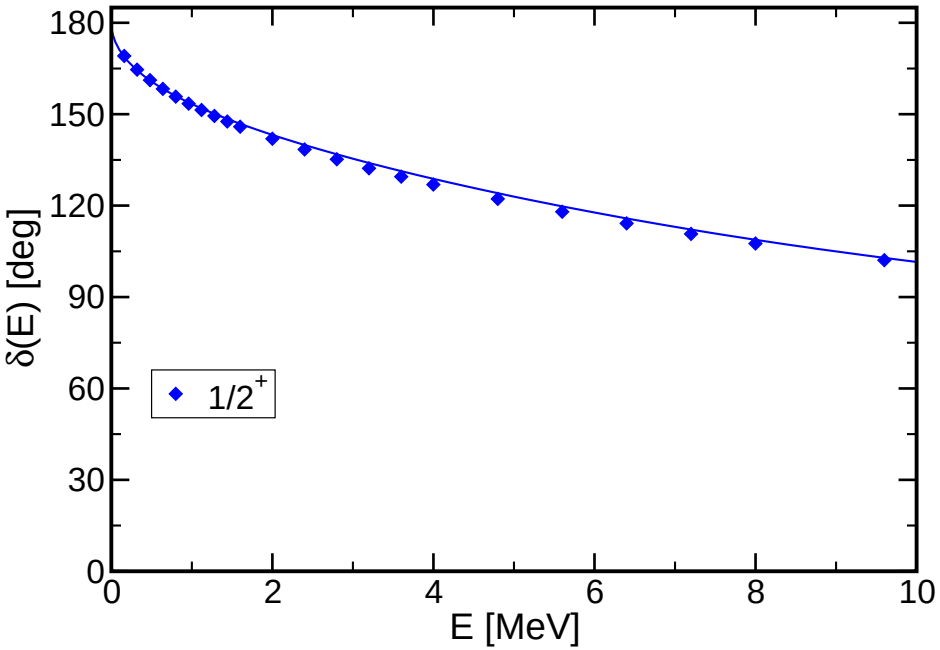

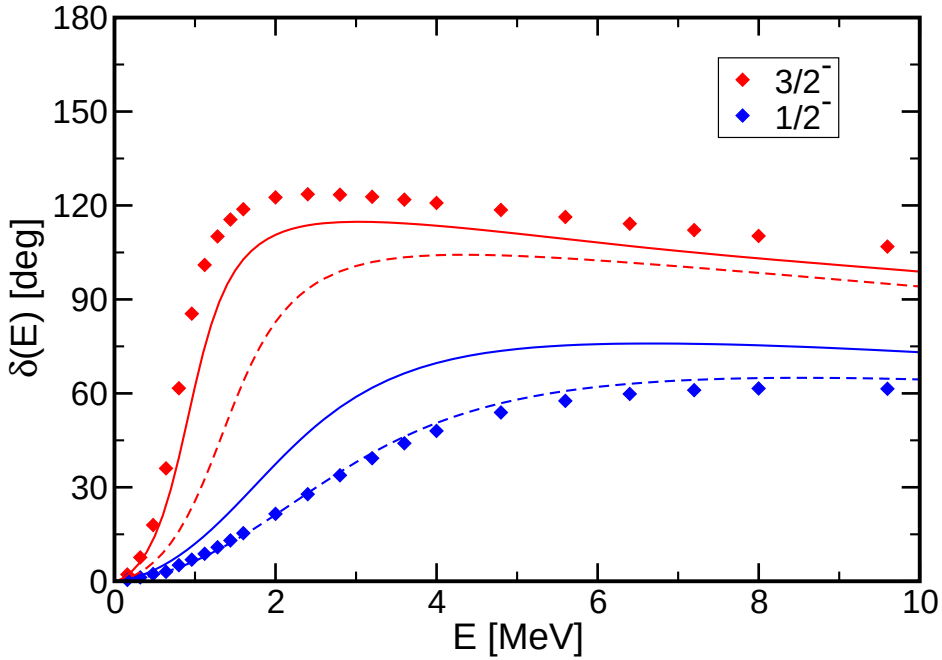

dashed lines – frozen configurations only, solid lines – polarized configurations included

- UCOM(SRG) interaction
- FMD VAP ($1/2^+$, $3/2^-$, $1/2^-$) plus radius constraint configurations in interaction region

➥ polarization effects very small in *S*-wave scattering

➥ splitting between $3/2^-$ and $1/2^-$ states too small –
consistent with GFMC (two-body interaction only) and NCSM results

^{4}He-^{4}He scattering

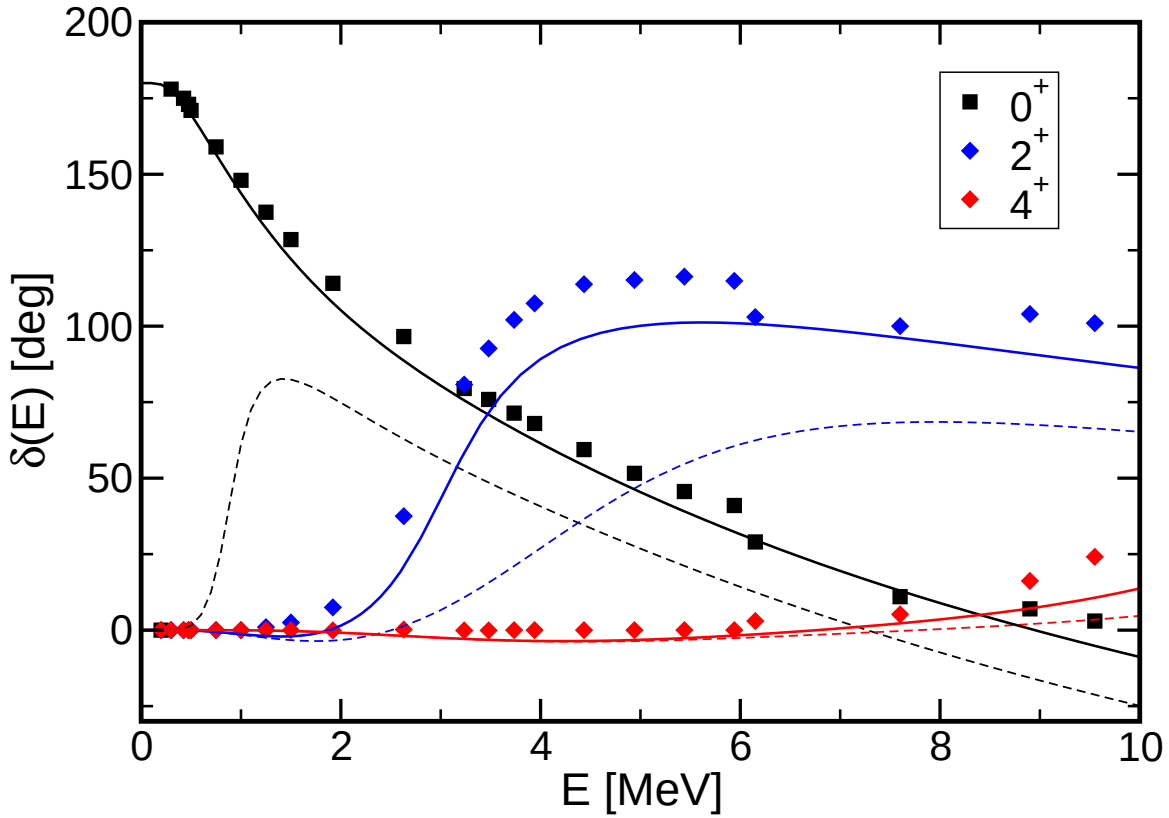

- UCOM(SRG) interaction
- FMD VAP (0^+, 2^+, 4^+) plus radius constraint configurations in interaction region

➥ polarization effects shift *S*- and *D*-wave resonances by about 1 MeV

Summary

Unitary Correlation Operator Method

- Explicit description of short-range central and tensor correlations
- Realistic low-momentum interaction V_{UCOM}
- NCSM calculations with UCOM

Fermionic Molecular Dynamics

- Microscopic many-body approach using Gaussian wave-packets
- Projection and multiconfiguration mixing

^{3}He(α,γ)^{7}Be Radiative Capture

- Bound states, resonance and scattering wave functions
- S-Factor: energy dependence and normalization
- Analyzed in terms of overlap functions
- Inconsistency of ^{3}He(α,γ)^{7}Be and ^{3}H(α,γ)^{7}Li data ?

Thanks to my collaborators:
Hans Feldmeier (GSI), Wataru Horiuchi (RIKEN), Karlheinz Langanke (GSI),
Robert Roth (TUD), Yasuyuki Suzuki (Niigata), Dennis Weber (GSI)